



# European daily dataset of soil moisture from *in situ* meteorological observations

Gerard van der Schrier<sup>1</sup>, Milan Fischer<sup>2,3</sup>, Martin Mulder<sup>4</sup>, Jos van Dam<sup>4</sup>, Jan Řehoř<sup>2,5</sup>, and Miroslav Trnka<sup>2,3</sup>

<sup>1</sup>Royal Netherlands Meteorological Institute, De Bilt, the Netherlands

<sup>2</sup>Global Change Research Institute, Czech Academy of Sciences, Brno, Czech Republic

<sup>3</sup>Department of Agrosystems and Bioclimatology, Mendel University in Brno, Brno, Czech Republic

<sup>4</sup>Department of Environmental Sciences, Wageningen University and Research Centre, Wageningen, The Netherlands

<sup>5</sup>Institute of Geography, Masaryk University, Brno, Czech Republic

**Correspondence:** G. van der Schrier (schrier@knmi.nl)

**Abstract.** This paper documents the development and validation of an *in situ* dataset for daily soil moisture based on observed meteorological variables from the European Climate Assessment & Dataset (ECA&D). These data are input to the SoilClim model which provides soil water contents values for the upper 10 cm, the root zone and the deeper layer of the soil. Soil characteristics are taken from the widely used SoilGrids system. The meteorological input data are daily precipitation totals, 5 daily averaged temperature, and global radiation sums. The pan-European dataset for soil water content results in a set of 5758 stations for which daily soil water content values are produced, for the surface zone (upper 10 cm) and for the root zone (upper 40 cm), for the period for which all input data is available. Model results are validated against observations of actual evapotranspiration ( $ET_a$ ) from the FluxNet experiment. Calculated soil water content are compared against a selection of the observations of the International Soil Moisture Network (ISMN). In the comparisons against observations, calculated 10 values of  $ET_a$  and soil water content (SWC) from the state-of-the-art soil dynamics model SWAP, which is more advanced than SoilClim, are used as well. The comparisons show that SoilClim and SWAP show generally the same behaviour albeit that SoilClim saturates quicker than SWAP. On average, the similarity between the models and observation for  $ET_a$  is higher (correlations 0.77 and 0.78 for SWAP and SoilClim respectively) than for the observed soil water content, where average correlations for the surface and rootzone vary between 0.52 and 0.62.

15 Based on the rootzone soil water content, four climate indices are calculated. These are the Soil Moisture Index (SMI) which is a metric to compare soil water content values across the diverse climatic zones which are present in Europe. This index relates to water content levels that are above or below the 50% level of the field capacity. In addition, an index is introduced that simply counts the number of days where the soil water content drops below the 50% level of the field capacity. In addition, two indices assess more extreme soil water content values: the number days where the soil water content is either nearly at field capacity or 20 close to the wilting point. The 1991-2020 spring and summer climatology is provided for this dataset in terms of these indices. The relatively recent 2018 drought is put in a historical perspective by a comparison against the 1976 drought and a trend analysis of summer desiccation since 1979 is provided.



The use of *in situ* observations, the daily resolution and the climate indices included in the described dataset make it suitable as validation of other soil moisture datasets and the assessment of changes in the occurrence of extremes in soil moisture over the European domain. The dataset of daily soil moisture from *in situ* meteorological observations is available at <https://doi.org/10.21944/phk8-at71> (van der Schrier et al., 2026).

## 1 Introduction

Northwest Europe has recently seen three consecutive springs and summers that have been dry and sunny (2018, 2019, 2020). In between these seasons, the autumn and winters failed to compensate for the shortage of water. This has led to widespread water availability issues. Van der Wiel et al. (2023) indicate that such multi-year droughts are expected to occur more often in a warming climate, with the resulting feed-back on heatwaves as we have recently seen (Lemus-Canovas et al., 2024). An early example where successive dry and (for spring and summer) sunny seasons have led to a severe drought is the 1921 drought (van der Schrier et al., 2021), which resulted in a drought that is still the severest on record (van der Schrier et al., 2006). While droughts are among the costliest climatic extremes, excessively wet periods can be equally problematic from the perspective of a farmer when fields are too wet for harvesting and crops perish. Especially in the northern half of Europe, where the annual sum of precipitation is increasing, and wet autumns have occurred more often in recent decades (Kendon et al., 2024). The 12-month period until the end of the 2024 spring stands out in this respect as it has been the wettest 12-month period since records began in parts of Central Europe (Tagesspiegel, 2024; KNMI, 2024). Recurring droughts and pluvials are aspects of climatic change that have a large societal relevance but our ability to monitor the impacts of these climatic events is limited. The common approach is to use standard drought indices like SPI, SPEI and scPDSI which are all based on atmospheric parameters only and, for the SPEI and scPDSI, make attempts to capture the loss of moisture from the soils to atmosphere too. A comprehensive review of drought indices can be found in Heim (2002). All these indices are used as proxies for soil water content but the dynamics of soil water content is not or only very rudimentary captured in these indices. The time scale at which these drought indices are usually calculated - monthly - is too coarse to monitor short term variations in the soil water balance. It also ignores the climate change-related shift in the distribution of daily precipitation towards longer dry spells and more extreme precipitation (Kysely, 2009; Zolina et al., 2010; Cavanaugh et al., 2015). Extreme precipitation produces larger runoff and smaller infiltration of moisture into the soil, which further decouples precipitation amount from soil moisture content. The shift in the precipitation distribution impacts soil moisture which is not captured when using monthly mean values. It is the soil water balance that needs to be resolved to address short-term fluctuations, like flash droughts (spells of extreme heat that are related to a lack of soil moisture) and floods that occur when strong rains are combined with saturated soils.

The importance of soil moisture in climate dynamics contrasts with the lack of *in situ* observational datasets for soil water content. There are several consequences of this omission. One is that alternative sources for soil moisture information, like the ERA5 Land (Muñoz Sabater et al., 2021) and the C3S Soil Moisture satellite dataset (Dorigo et al., 2019), lack a continent-wide validation dataset. For the assessment of the annual soil moisture anomaly in the 2019 European State of the Climate (C3S, 2020), which had a summer where many national heat records were broken, this produced a view on soil moisture anomalies



that was not entirely consistent between these two products. Focusing on the Mediterranean region, a lack of a uniform and consistent validation dataset for soil water content interferes with that region's vulnerability to soil moisture deficits. Recently Ardilouze et al. (2022) argued that a model analysis of the soil moisture - precipitation feedback in the Mediterranean is hampered by a 'wide array of uncertainties', pointing to soil moisture and its representation in climate models.

60 Observational sites for soil moisture are costly to set-up and to operate. The consequence is that only a few ground-based soil moisture measurement networks are available (Robock et al., 2000). Except of a few long-running stations, like those in the Ukraine (Robock et al., 2005), the records are usually short. The poor availability of ground observations for soil moisture which is limiting progress in these disciplines (Seneviratne et al., 2010), has been the motivation to construct an observation-based dataset for soil water content. Here, we document the construction and validation of a dataset of daily values of soil  
65 moisture for Europe based on observed *in situ* daily values of precipitation, temperature, global radiation and observed soil characteristics which force the soil moisture model SoilClim (Hlavinka et al., 2011).

The network of meteorological stations used in this dataset is that of the European Climate Assessment & Dataset (ECA&D, Klein Tank et al. (2002)) and the meteorological data are owned and provided by the European National Meteorological Services (NMSs). The use of these quality controlled meteorological observed quantities has the benefit that it makes use of  
70 the dense network and the full historical records of these observations. In addition, the World Meteorological Organization (WMO, WMO (2023)) prescribes that these stations are situated over short-clipped grass and should be representative for a wider region. This has the benefit that a certain standardisation in drought monitoring is in place. The drawback is that soil moisture information for other land uses, like forests and agricultural crops, is missing in this dataset.

Specific for soil moisture monitoring purposes, a set of soil moisture indices is used based on the rootzone soil moisture  
75 content, which aims to provide a historical perspective of soil water content variations. These indices are taken either from the literature, like the Soil Moisture Index proposed by Hunt et al. (2009) which draws upon earlier suggestions (Betts, 2004). Inspired by the climate impact indices of the WMO Commission for Climatology's Expert Team on Sector-specific Climate Indices (ET-SCI), soil water content indices are added that monitor the occurrence of more extreme conditions. These relate to the number of daily occurrences of moisture stressed, very moisture stressed or very moisture saturated conditions.

80 The calculation of soil water content for this dataset is based on the SoilClim model (Hlavinka et al., 2011). There are more complex models for water balance estimates in a soil-crop system available, like the SWAP model (Kroes et al., 2017; Heinen et al., 2024), but that requires detailed or specialized input data (e.g. water retention function, hydraulic conductivity function, root density and other inputs). The motivation to use SoilClim is that it can be used for a wide range of climatic conditions, it requires a modest amount of input data and it has low computational costs. In this study, the SoilClim is validated against  
85 observations of actual evapotranspiration, a selected set of soil moisture observations, and it is compared against SWAP model results where both soil moisture models are forced with similar input data.



## 2 Data and Methods

### 2.1 ECA&D

The European Climate Assessment & Dataset (ECA&D) is a repository of meteorological station records for Europe with the purpose providing a platform with easy access to high quality *in situ* observations. In addition, derived data products are produced to monitor climatic change and variations. The long records in ECA&D give the historical perspective to recent climatic extremes. The data collated by the ECA&D initiative are mostly supplied directly by the European NMSs. For the countries outside the European Union the number of stations available to ECA&D may be a subset of the complete network available to the NMSs. This is due to restrictions concerning the exchange of data. Other sources of data are repositories that, similar to ECA&D, aim to provide unified access to a large set of data. The original source of these data is the NMSs as well.

ECA&D is the backbone of the Climate Data node for the WMO Regional Climate Centre for Europe and the Middle East. The domain covered is referred to as Regional Association (RA) VI.

ECA&D collaborates with regional meteorological services, like the Meteorological Service of Catalonia in Spain, environmental services, like the ARPA's (Regional Environmental Protection Agencies) in Italy or river authorities like those in Flanders and Walloon. Universities and observatories share their data with ECA&D as well, like the Armagh Observatory in Northern Ireland, the Radcliffe Meteorological Station of Oxford University in England or the data gathered by the Wageningen University in the Netherlands. In some countries, data are supplied by both the NMS and from an complementary network through the ministry of agriculture, like in Luxembourg and Portugal.

Figure 1 shows the spatial and temporal availability of rain gauges, stations that provide daily averaged temperature and stations providing global radiation. These are the meteorological variables that are required in the calculation of soil moisture content. The figure shows the large amount of station data in the western half of the continent, with the number of rain gauges outnumbering by far stations that provide daily averaged temperature. The number of stations that provide global radiation values is clearly the smallest and the availability of the latter variable is the bottleneck in further expanding the dataset with soil moisture content.

Figure 2 illustrates the availability of stations for which soil moisture data can be provided. The total number of stations in this map is 5758. The number of stations provided through other sources than directly through the NMS varies depending on the variables. For daily precipitation and average temperature, the percentages of data not directly provided by the NMSs are 5.05% and 6.06% respectively. In contrast, for global radiation this percentage is 13.28%. The strong contribution of the European NMSs to ECA&D parallels their increasing willingness to share data more abundantly. This is fuelled by efforts of the World Meteorological Organization to urge member states to share data (WMO, 2022) and EU regulations 2019/1024 and 2023/138 on Open Data and re-use of public sector information and, more specifically, on Meteorological data (EU Commission, 2022). Nevertheless, the efforts of organisations to build large and consistent repositories with *in situ* data have been used



to supplement data for global radiation, where the data from the European domain of the World Radiation Data Centre<sup>1</sup> and the Baseline Surface Radiation Network (BSRN)<sup>2</sup> (Driemel et al., 2018) are shared with ECA&D.

120 Any gaps in the time series provided to ECA&D are filled with data from neighbouring series to form more temporally complete series (ECA&D Project Team, 2012; van der Schrier et al., 2013). To update the series to near real time when updates of the NMSs are not available, data are used from synoptic messages (SYNOP) distributed via the Global Telecommunications System WMO (2007). The SYNOP data are replaced when validated data become available from the NMSs (van den Besselaar et al., 2012).

125 A range of different methods is used to calculate the daily values, and this is often dependent upon the convention used by a given data provider. For example, daily mean temperatures may be the average of maximum and minimum temperatures, or may be the average of hourly readings, or another frequency such as three hourly. In addition, the start and end times of the 24h period over which elements are measured are not standardized across Europe and the date attached to each observation may sometimes be the end of the observation period rather than the start. Although no attempts are made to adjust for this

130 inhomogeneity across Europe, ECA&D staff apply a day shift when necessary to make sure that the observed period coincides as much as possible with the date attached to the observation (ECA&D Project Team, 2012).

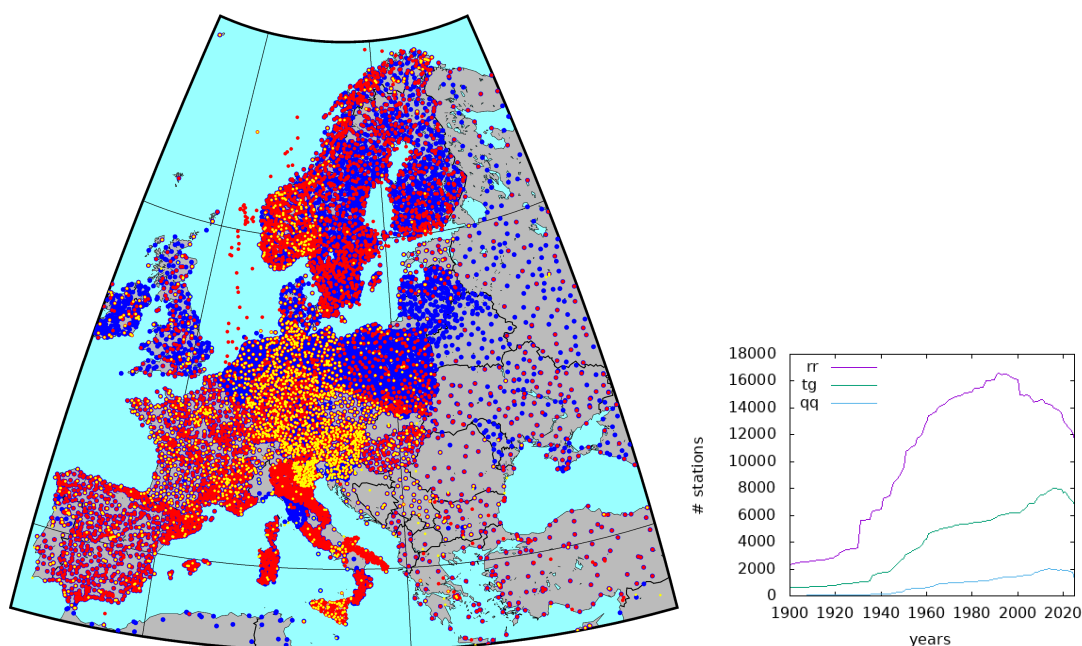


**Figure 1.** Map of the locations of rain gauges (blue) and stations recording daily average temperature (red) and global radiation (yellow) in ECA&D (left). The coloured dots are overlain with varying sizes to make clear that many stations provide all three variables. The right plot shows the temporal evolution of the number of rain gauges versus the number of global radiation stations since 1900.

<sup>1</sup><http://wrdc.mgo.rssi.ru>

<sup>2</sup><https://bsrn.awi.de>

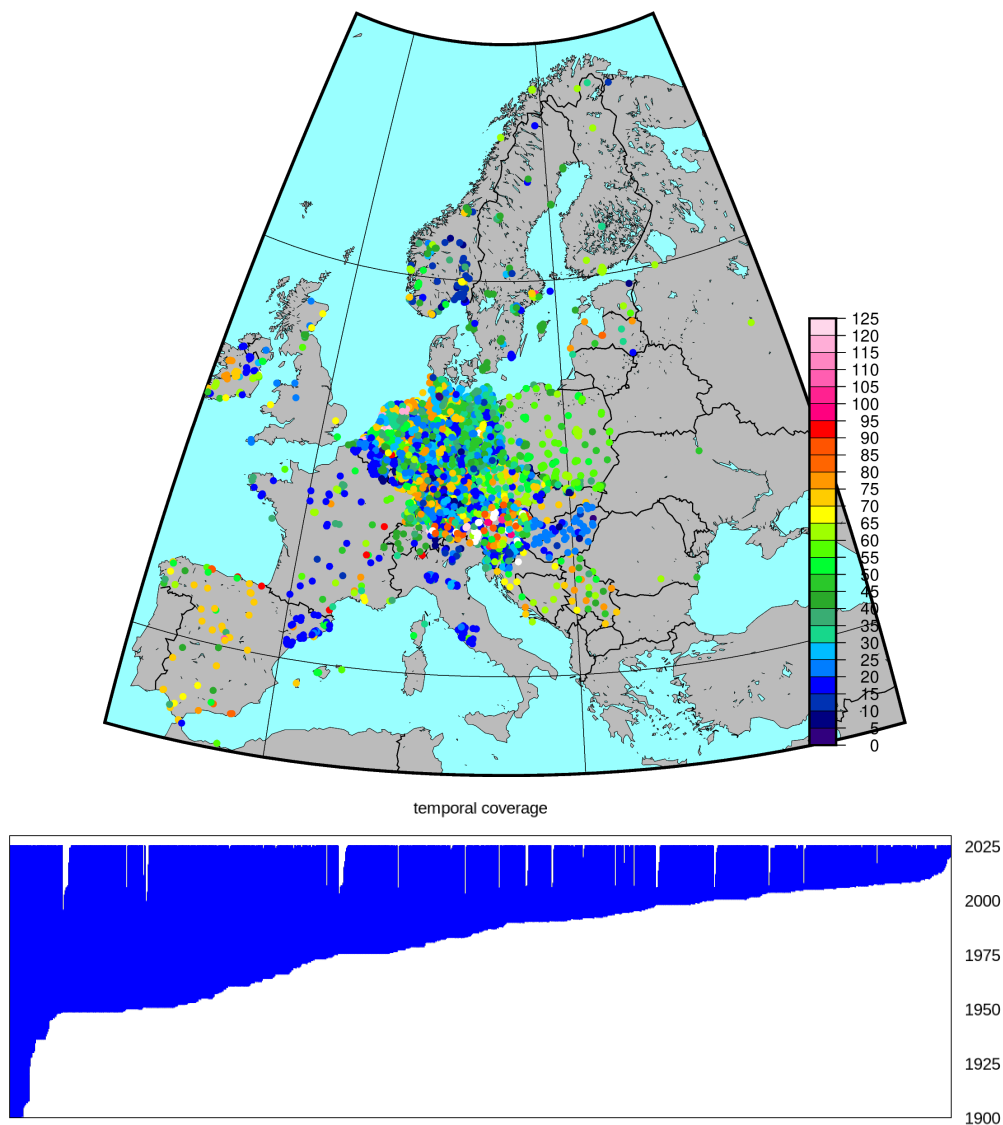


**Figure 2.** Locations for which soil moisture can be calculated using in meteorological situ data from ECA&D and soil characteristics. The colour coding shows the length of the soil water content timeseries in years. The bottom panel shows the start and stop dates of the available soil water content series on the vertical axis, the horizontal axis shows a simple ordering of the series by start date.

## 2.2 The land use and soil characteristics dataset

### 2.2.1 Land use

The selection of validation data is based on the type of land use present at the observational site. This is motivated by the observation that by far most of the meteorological stations that are provided by the NMSs to ECA&D have a specified land use.



The World Meteorological Organization prescribes that these stations are situated over short-clipped grass and be representative for a wider region. This gives a natural way to select stations in the validation against observed data; only those stations in the verification dataset that are situated over grassland are included in the verification. To expand the set of verification stations, we include stations over rainfed crop as well. Information on land use is sourced from the C3S Land Cover project.

140 The C3S Land Cover project delivers the global Land Cover maps at  $0.002778^\circ$  spatial resolution (approximately 300 m at the equator) for 2016 to 2020 (version 2.1). These data are cropped to include only Europe. The dataset is a product of the ESA Climate Change Initiative (Bontemps et al., 2013).

The typology was defined using the Land Cover Classification System (LCCS) developed by the United Nations' Food and Agriculture Organization, aiming to be as much as possible compatible with the GLC2000, GlobCover 2005 and 2009 products.

145 In addition, the UN-LCCS was found to be compatible with the Plant Functional Types used in climate models (ESA, 2011) The UN-LCCS defines land cover classes using a set of classifiers.

### 2.2.2 Soil characteristics

Data for the soil characteristics is from the SoilGrids system (Hengl et al., 2017), which provides provides global estimates for standard numeric soil properties (organic carbon, bulk density, Cation Exchange Capacity (CEC), pH, soil texture fractions and coarse fragments) at six standard depths (0–5, 5–15, 15–30, 30–60, 60–100 and 100–200 cm). The original data is provided at  
150 250 m resolution in the equidistant Equi7 Grid. For the application discussed here, the projection was remapped to a standard WGS84 grid and confined to the WMO RA VI domain.

In the construction of the soil maps, Hengl et al. (2017) used the most detailed 30 m resolution global land cover map from 2010. This was combined with a global water mask and a global sea mask map to produce one consistent global soil mask that  
155 includes all land areas. For urban areas, soil characteristics are not available in SoilGrids. In ECA&D, there are a few stations in the heart of Europe's major cities and many stations are close to urban development. In addition, the accuracy of the location metadata of meteorological stations is not always at the same detail at which the SoilGrids data is provided due to e.g. the protection of the privacy of operators of manual rain gauges, which might make the location of a station on the SoilGrids maps coincides with a 'missing' value. To circumvent this problem, a nearest neighbour infilling is applied for all 'missing' values  
160 in the SoilGrids maps.

### 2.3 Reference evapotranspiration

The Penman-Monteith parameterization for reference evapotranspiration  $ET_0$  is the scientific standard as it is generally considered to be the most physics-based description of reference evaporation  $ET_a$ . However, it is applied while disregarding the assumption of well-watered surrounding the station, so that the meteorological observations used for the parameterization are in  
165 equilibrium with the surroundings. We note that these assumptions are generally not met, and that when the public interest for information on  $ET_0$  increases - during times of drought - the suitability of the parameterization decreases. Also representative daily values on wind speed and air humidity, which are required by the Penman-Monteith equation, are not available at many weather stations. A parameterization that is much less demanding on the amount of input data and more straightforward to ap-



ply, is the one proposed by Makkink (Makkink, 1957; de Bruin, 1981; de Bruin and Holtslag, 1982; de Bruin, 1987; de Bruin  
170 and Stricker, 2000), which recognizes (similar as Penman did) that radiation is the principal driver for evapotranspiration. The  
formula used is:

$$E_r = C \frac{s}{s + \gamma} \frac{K}{\lambda}, \quad (1)$$

where  $E_r$  is the reference crop evapotranspiration,  $C$  a constant with the value 0.65,  $s$  the slope vapour pressure,  $\gamma$  the psy-  
175 chometric constant with the value 0.067 kPa/°C,  $\lambda$  the latent heat of evaporation, and  $K$  the global radiation. This (simplified)  
version of Makkink's formula is used as it only needs global radiation and air temperature as input. Sea level air pressure is  
input to the psychrometer constant, but the impact of pressure variations is very small and can be ignored for practical purposes.  
Makkink adds the ambient air temperature to account for the Clausius–Clapeyron change in the uptake of water vapour in air as  
temperature changes. This simpler approach is underpinned by the study of Maes et al. (2019) who use eddy-covariance mea-  
180 surements from the FLUXNET2015 database to parameterise and inter-compare some of the various methods available. They  
found that a simple radiation-driven method, calibrated per biome, consistently performs best against *in situ* measurements.  
A Priestley-Taylor method, where radiation and temperature are combined as in the Makkink method, performed just slightly  
worse but substantially and consistently better than the Penman–Monteith parameterization. A similar conclusion was reached  
earlier in a comparison of the Makkink and Penman–Monteith parameterizations at a research facility in the Netherlands over  
the exceptionally dry year 1976 (de Bruin, 1981; de Bruin and Holtslag, 1982).

185 The value of the psychometric constant in eq. 1 is assumed to be uniform over Europe. This is motivated by the similar  
assumption for the constants on the FAO-based Penman-Monteith parametrization Allen et al. (1994).

The use of a method combining radiation and temperature, rather than one which is based on radiation alone, is motivated  
by the provision of the long historical perspective in the soil moisture record of this study. For this purpose, both the trend in  
radiation and the trend in air temperature need to be considered.

## 190 2.4 The soil moisture models

### 2.4.1 The SWAP model

SWAP (Soil-Water-Atmosphere-Plant) simulates water transport, solutes and heat in the vadose zone in interaction with vege-  
tation development (Kroes et al., 2017). In the vertical direction the model reaches from the canopy to the shallow groundwater  
which makes SWAP a one-dimensional vertically directed model.

195 The Richardson equation is used to calculate the soil flow in layered soil profiles. The Mualem-Van Genuchten relations  
describe the soil hydraulic functions of each soil layer, where a modification of these equations is used near saturation. Finally,  
the bottom boundary used in our study is free drainage.

The daily input of leaf area index, rooting depth and root density are used to compute the crop development rather than the  
actual weather and hydrologic conditions. The crop inception of moisture is calculated using the scheme of Von Hoyningen-  
200 Hüne and Braden. In this study, Makkink reference evapotranspiration with the crop factor of shortly clipped grass is used to



	SWAP	SoilClim	source
water flow			
daily evapotranspiration	+	+	ECA&D
daily rainfall	+	+	ECA&D
soil hydraulic properties	+	-	SoilGrids
drainage conditions	-	-	SoilGrids

**Table 1.** Listing of required input for the SWAP and SoilClim models.

calculate potential evapotranspiration (Makkink, 1957). Actual transpiration depends on the moisture and salinity conditions in the root zone, weighted by the root density. Actual evaporation depends on the hydraulic capacity of the soil to transport water to the soil surface (Kroes et al., 2017).

Surface runoff will be calculated when the height of the water ponding on the soil surface exceeds a critical height. The rate of surface runoff depends on a specific runoff resistance.

The snow model calculates the accumulation and melting of a snow pack as a function of air temperature in relation to a threshold value. This models the growth of the snow pack by snowfall and rain, and the decline by snow melt and sublimation. Adjustments to the soil-snow heat flux and soil temperature follow in the presence of snow pack.

#### 2.4.2 The SoilClim model

The SoilClim model simulates soil water balance, soil temperature, actual ( $ET_a$ ) evapotranspiration and the presence of snow cover. The method for water balance estimates is proposed by Allen et al. (1998) which was modified and integrated with a snow cover model and a soil temperature model (Hlavinka et al., 2011). SoilClim calculates the soil water and temperature dynamics with a daily time stepping. The meteorological input are daily sums of precipitation, temperature and reference evapotranspiration. Other input is basic information about the soil properties and vegetation cover. The implemented SoilClim setup considers four soil layers (0.0–0.1, 0.1–0.4, 0.4–1.0 and 1.0–2.0 m) and calculates soil moisture based on the relationship between inflow (water infiltration) and outflow (evapotranspiration and deep percolation) water-balance components (Hlavinka et al., 2011).

SoilClim accounts for the snow cover accumulation and melting, allowing more precise water balance estimates in the areas where snow cover represents a significant portion of the annual precipitation total. The presence of snow cover, its accumulation (in mm of equivalent water) and melting were estimated based on the Snow- MAUS model (Trnka et al., 2010), which operates with a daily time step with maximum and minimum air temperatures and daily sums of precipitation as input. The Snow-MAUS model compares well with more sophisticated snow models (Hlavinka et al., 2011).

The difference in complexity between SWAP and SoilClim is partly reflected in the amount of input data that is required. Table 1 compares the input requirements between these models, where the capabilities of SWAP to model solute flow and crop development (which require additional input data) are not used.



### 2.4.3 Groundwater level

Although both the SWAP and SoilClim models have the possibility to account for the interaction of soil moisture with the groundwater level, the dynamics of groundwater level is not included in this dataset. Groundwater levels fluctuate due to seasonal changes, precipitation, irrigation, and land use. Capturing these dynamics accurately requires high-resolution temporal and spatial data. Such data is not available for the pan-European domain which motivates the approach to exclude groundwater information in the soilmoisture calculations. For areas where the groundwater level is relatively high, the calculated soilmoisture values will be less accurate. Figure 3 illustrates the climatological groundwater table depth in February and August for Europe based on the global analysis of Fan et al. (2013). Groundwater levels deeper than -6 m are set to -6 m and the colour scale distinguishes between depth below -3 m, for which ignoring any ground water effects on surface and root-zone is acceptable, and less deep groundwater table levels. The areas with a more shallow groundwater table are in the Low Countries (Netherlands, north-west Germany and parts of Flanders), the area around The Wash in the UK, the Po valley in Italy, the coastal region south-east of Sevilla, Spain, the Danube and its delta and the plains in central Europe. In August, the groundwater tables in these regions are a bit deeper and the extent of the regions is slightly smaller than in February.

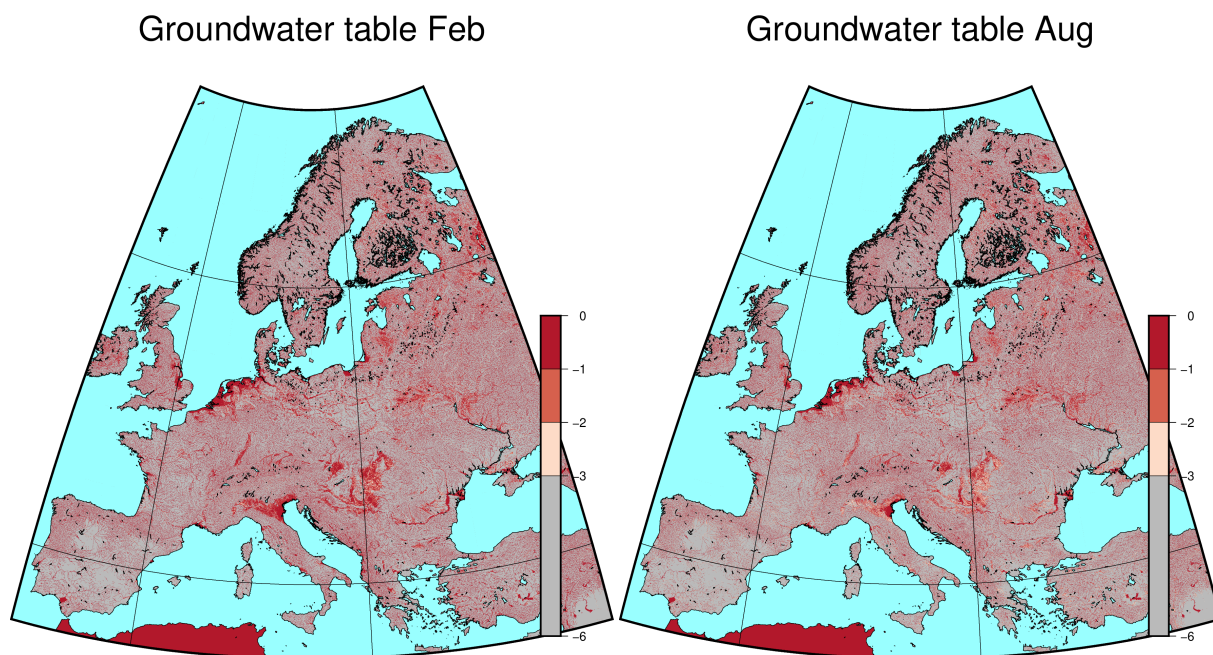


**Figure 3.** Groundwater table depths for February and August based on the analysis of Fan et al. (2013). Lower depth tables than -3 m are grey, groundwater tables that are less deep are in shades of red.



---

AW10p	number of days when the Soil Water Content < 10% of maximum Available Water Content Let $AW_{ij}$ be the daily soil water content on day $i$ in period $j$ and let AW10 be the 10% value of the maximum Available Water Capacity. The index in the period $j$ is determined by counting days where $AW_{ij} < AW10$ .
AW90p	number of days when Soil Water Content > 90% of maximum Available Water Content Let $AW_{ij}$ be the daily soil water content on day $i$ in period $j$ and let AW90 be the 90% value of the maximum Available Water Capacity. The index in the period $j$ is determined by counting days where $AW_{ij} > AW90$ .
SMI	Soil Moisture Index Based on actual water content and a known field capacity and wilting point, the SMI is a continuous function and is scaled from 5.0 to -5.0, with 5.0 representing water content at field capacity and -5.0 representing water content at wilting point. SMI represents the time mean value.
SMIO	number of days with moisture stress Let $SMI_{ij}$ be the daily Soil Moisture Index on day $i$ in period $j$ . The number of days in period $j$ is determined by counting the days where $SMI_{ij} < 0$ .

---

**Table 2.** Definition of climate indices for soil water content.

## 2.5 Climate indices

240 An index specifically designed for soil moisture monitoring is the Soil Moisture Index (SMI) (Hunt et al., 2009) This index  
can identify a quick onset of agricultural drought by comparing the observed dryness of a soil relative to the plant's ability  
to extract water. Hunt et al. (2009) explain the rationale behind the SMI with the observation that actual evapotranspiration  
became limiting halfway between field capacity and wilting point. The SMI is defined such that positive values correspond to  
the situation that soil moisture is above the 50% threshold of total available water and negative SMI values correspond to the  
245 situation that soil moisture is below that threshold. An SMI value of 0 separates the stress versus the non-stress situations. For  
the current purpose, SMI is calculated for every day and aggregated values are presented. To highlight the frequency of days  
where soil moisture stress kicks in, the number of days per period where the daily SMI values drop below 0 is calculated and  
presented as index SMIO.

Indices that focus more on the extreme cases of moisture stress or moisture saturated situations are the AW10p and AW90p  
250 indices, respectively. These indices calculate the number of days in each period where soil moisture is close to the wilting  
point or close to the field capacity. A more detailed definition is given in table 2 and the indices are schematically illustrated  
in fig. 4. In the phase space of soil water content values and the fineness of soil texture, possible values of soil water content  
are limited by the wilting point and the field capacity. When soil water content is in purple or green areas in the plot, indices  
AW90p and AW10p respectively become non-zero. Index SMIO gets larger the more days soil water content is in the blue area.  
255 SMI indicates where, on average over a specified period, soil water content is found in this diagram.

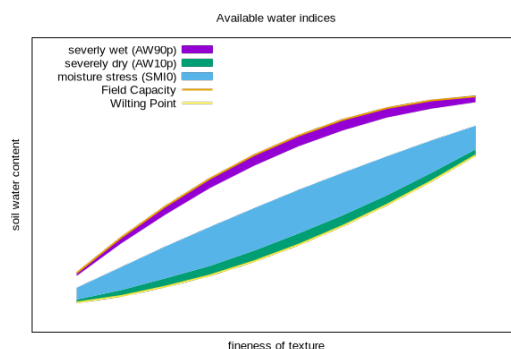


**Figure 4.** Schematic relationship between soil moisture and texture, with indications as to what the indices AW10p, AW90p and SMIO relate to. Figure inspired by Barker et al. (2005, fig 1-6).

### 3 The operational embedding

#### 3.1 The selection of ECA&D stations

Soil moisture estimates require input data for the amount of precipitation and the reference evapotranspiration  $ET_0$ . The stations available in ECA&D may not have all required variables present at each location as networks with only rain gauges are included as well or if only part of the available variables are shared with ECA&D. The mismatch in density of the rain gauge network and those of temperature and radiation (Figure 1) did motivate us to use the approach described below. The basis for the calculations are the blended series as described in Sect. 2.1.

Starting with the full network of stations that provide daily precipitation, the closest stations in the neighbourhood (within 25km) that provides global radiation (QQ) data and a station that provides daily mean temperature (TG) are located. For the station that provides temperature, the additional requirement is added that the elevation difference with the rain gauge should be less than 250 m. These latter two stations often coincide, but that is not always the case. If these stations can be found, a search is made for the nearest station that provides sea-level pressure (SLP). If no SLP-providing station can be found in the neighbourhood, the standard atmospheric pressure of 1030hPa is used as the influence of air pressure on  $ET_0$  values is very small. With the daily values of QQ, TG and SLP, daily values of the Makkink reference evapotranspiration  $ET_0$  can be calculated (Sect. 2.3).

The limiting factor in terms of the network density for which soil moisture can be calculated is the number of global radiation stations. The collection of global radiation records and the transformation of sunshine duration to global radiation records, the former often go further back in time. The transformation from sunshine duration series to global radiation series is done following the approach of Suehrcke et al. (2013). To illustrate this point, the number of rain gauges available in ECA&D (irrespective of stop and start dates) is 20210. For daily mean temperature this value is 9100 while for global radiation the number is 2307 (status summer 2025). The argument to start the selection of ECA&D stations with the precipitation station



is that precipitation has a much shorter decorrelation length than daily mean temperature or daily values of global radiation which are much more spatially homogeneous in comparison to precipitation.

### 3.2 The selection of the soil characteristics

280 For the subset of precipitation stations that can be linked to neighbouring stations that provide the input for the reference evapotranspiration  $ET_0$ , the coordinates are used to extract the soil characteristics for the grid square that corresponds to that location. The soil hydraulic functions are derived following Wösten et al. (1999) where the Mualem - van Genuchten parameters ThetaR, ThetaS, Alpha, n, Tort and Ksat are determined from sand, silt, clay, bulk density, organic carbon content values sourced from the SoilGrids system (Hengl et al., 2017).

285 The Available Water Content (AWC) needs to be corrected for the amount of stones in the soils. This is done by

$$AWC = (1 - gravel)(FC - WP) \quad (2)$$

where *gravel* is the volume fraction of stones in the soils and *FC* and *WP* are the Field Capacity and Wilting Point.

In the calculations of soil water content in the soils, the actual groundwater table is ignored. Although Fan et al. (2013) present global observations of water table depth compiled from government archives and literature, a pan-European view on  
290 the actual groundwater table, updated in near-real time as is required for the current dataset, is not available. Therefore we apply both in SoilClim and SWAP free drainage. For SWAP, the model is initialized with the pressure head of each compartment in hydrostatic equilibrium with the initial groundwater level, which is set at -200 cm below soil surface.

### 3.3 Surface and root-zone soil moisture content

The WMO Essential Climate Variables for soil moisture are ‘Surface soil moisture’ and ‘Root-zone soil moisture’ (?) which is  
295 the motivation to include these two variables in the dataset. The output of the SoilClim model of the upper layer represents the soil moisture of the 0–10 cm layer. This is taken to be representative of the surface soil moisture. The study of Jackson et al. (1996, their fig.1) shows that 83% of the root biomass of temperate grassland is in the upper 30 cm of the soil. This motivates us to relate the soil moisture in the upper two layers of SoilClim (0–40 cm) to the root-zone soil moisture.

An additional motivation to provide both the surface and root-zone soil moisture content relates to the temporal variability  
300 of these two layers. Under dry conditions, the surface layer gradually decouples from the lower layer (Hirschi et al., 2014) and in in-situ observations show that the surface layer will then have a lower soil moisture content and variability compared to the root-zone layer.



siteid	name	lat	lon	elev	start	stop	surface
AT-Neu	Neustift	47.1167	11.3175	970	2002	2012	grass
BE-Lon	Lonzee	50.5516	4.7462	167	2004	2014	crop
CH-Oe1	Oensingen grassland	47.2858	7.7319	450	2002	2008	grass
CZ-BK2	Bily Kriz grassland	49.4944	18.5429	855	2004	2012	grass
DE-Geb	Gebesee	51.0997	10.9146	162	2001	2014	crop
DE-Gri	Grillenburg	50.9500	13.5126	385	2004	2014	grass
DE-Kli	Klingenberg	50.8931	13.5224	478	2004	2014	crop
ES-LJu	Llano de los Juanes	36.9266	-2.7521	1600	2004	2013	crop
ES-LgS	Laguna Seca	37.0979	-2.9658	2267	2007	2009	shrub
ES-Ln2	Lanjaron-Salvage	36.9695	-3.4758	2249	2009	2009	shrub
FI-Jok	Jokioinen	60.8986	23.5134	109	2000	2003	grass
FI-Let	Lettosuo	60.6418	23.9595	111	2009	2012	crop
FR-Gri	Grignon	48.8442	1.9519	125	2004	2014	crop
IT-MBo	Monte Bondone	46.0147	11.0458	1550	2003	2013	grass
NL-Hor	Horstermeer	52.2403	5.0713	2.2	2004	2011	grass

**Table 3.** Names and start & stop dates of FluxNet records. Surface coverage information is from Teuling et al. (2010) and from the ESA landsurface classification.

## 4 Verification

### 4.1 Verification against FluxNet

305 The SWAP and SoilClim models output actual evapotranspiration  $ET_a$  data when calculating the soil moisture profile. These data are generated for a selection of stations from the FluxNet initiative (Pastorello et al., 2020) as reference, using meteorological input data from the nearest ECA&D stations.

As the focus of the present study is on soil moisture records based on the meteorological records of the European NMHSs, the FluxNet stations that measure over grassland and rainfed crops are selected for this comparison as this is the prescribed surface coverage for WMO meteorological stations. The selection is partly based on earlier studies like the study of Graf et al. (2022), who analysed the energy partitioning across terrestrial ecosystems during the 2018 drought in Europe. This difference in response to heatwave in terms of heat balance between grass and forest land was described earlier by Teuling et al. (2010). The distinction in FluxNet stations for forest, grass, crop and marshes which is made by Graf et al. (2022), is used here as well. Table 3 shows the FluxNet stations over grass- and cropland which are used here for the validation of the soil moisture stations.

315 The variable used from the FluxNet dataset is latent heat with gapfilling (LE\_F\_MDS).

For the location of each selected FluxNet station, the nearest station which provides global radiation and temperature is located, the nearest rain gauge is located and the nearest station that provides SLP. These three locations can point to the same station, but as the networks for radiation, precipitation and SLP are very different in terms of density, this need not be the case. The SLP data is converted to station level pressure and is used for the psychrometric constant (Allen et al., 1994, their eq. 1.4). For some stations, this approach turns out to be rather unlucky. For instance the Czech Fluxnet station Bily Kriz is



coupled to the meteorological station Lysa Hora but the latter station is situated on the top of a mountain at 1323 m, it is an extremely leeward spot with precipitation of ca. 1500 mm / year and therefore likely to be not too representative of the wider surroundings.

Figure 5 shows scatter diagrams comparing the FluxNet data and the calculated SWAP and SoilClim data. Table 4 provides the (Pearson) correlation coefficient, the RMSE and the relative RMSE of the comparison. In terms of correlation, the modelled  $ET_a$  is not too far apart from the observed values; both SWAP and SoilClim correlate at 0.74. The difference between the models is shown in the RMSE and rRMSE values which are for SoilClim consistently higher than for SWAP. This indicates that SWAP calculates  $ET_a$  more closely than SoilClim for these stations.

The models overestimate the  $ET_a$  values in most cases, particularly for CZ-BK2 and FI-Jok. For station NL-Hor, some underestimation for the higher values of measured  $ET_a$  is present. For station IT-MBo, the complex topography and the difficulty in finding meteorological stations close to the observational site have resulted in a fairly large scatter.

Unfortunately, a comparison between observed and modelled  $ET_a$  for the three Spanish stations was not possible. The timeseries of  $ET_a$  for these stations showed a distinctly different behaviour in the dry season than what was modelled. The much higher observed values of  $ET_a$  in comparison to the modelled figures indicate an additional water source, like irrigation, than what is provided as rain in the nearby rain gauges.

The resemblance between the observed  $ET_a$  data for the selected Fluxnet stations and the modelled data using the nearest meteorological station is generally fair. The correlation is high, and where the correlation between observed and modelled  $ET_a$  is low, the similarity between the SWAP and SoilClim output is strong. This suggests that the poor correlation might be attributed to meteorological data that are not sufficiently representative for the FluxNet site.

Figure 6 shows the average seasonal cycle, the median and the range of values between the 25<sup>th</sup> and 75<sup>th</sup> percentiles of  $ET_a$  for four selected FluxNet stations and the SWAP and SoilClim simulations. The daily values of the median and percentiles are determined by combining all available data and by using a 31-day window centered around each calendar day to further increase sample size and smooth the seasonal cycle. These plots show that the seasonal cycle is reasonably well captured in the Austrian station, although there is some overestimation in the early part of the year. The miss-representation of the amplitude in summer for the Czech station is obvious in Figure 5 as well and is related to the awkward location of the meteorological station used for this comparison. Nevertheless, these figures confirm that both soil moisture models produce similar seasonal cycles in  $ET_a$  although differences with observed values exist.

## 4.2 Verification against ISMN

The International Soil Moisture Network (ISMN, Robock et al. (2000)) maintains a global in-situ soil moisture database. This initiative started as a community effort, funded by the European Space Agency, to serve as a centralised data hosting facility for globally available *in situ* soil moisture measurements (Dorigo et al., 2021, 2011). Similar to the comparison against FluxNet stations, ISMN stations for use in the validation are selected that are located in grassland or rainfed crop. In addition, the time series should have at least five years of data.



station	SWAP	SoilClim
	corr/RMSE/rRMSE	corr/RMSE/rRMSE
AT-Neu Patscherkofel (AT) / Patscherkofel (AT)	0.85/0.76/0.52	0.84/1.02/0.68
BE-Lon Maastricht (NL) / Perwez (BE))	0.74/0.84/0.78	0.81/1.01/0.93
CH-Oe1 Basel Binningen (CH) / Basel Binningen (CH)	0.86/0.69/0.41	0.85/0.82/0.49
CZ-BK2 Lysa Hora (CZ) / Lysa Hora (CZ)	0.77/1.19/1.88	0.75/1.54/2.43
DE-Geb Erfurt-Bindersleben (DE) / Erfurt-Bindersleben (DE)	0.77/0.81/0.74	0.77/0.91/0.83
DE-Gri Nossen (DE) / Tharandt-Grillenburg (DE)	0.83/0.81/0.76	0.85/1.07/1.00
FI-Jok Jokioinen Jokioisten Observatorio (FI) / Jokioinen Jokioisten Observatorio (FI)	0.76/0.98/1.28	0.78/1.41/1.84
FI-Let Jokioinen Jokioisten Observatorio (FI) / Jokioinen Jokioisten Observatorio (FI)	0.74/0.83/0.67	0.76/1.04/0.83
FR-Gri Trappes (FR) / Trappes (FR)	0.68/0.85/0.61	0.69/0.95/0.68
IT-MBo Obergurgl (AT) / Aldeno (IT)	0.59/1.19/0.76	0.57/1.27/0.81
NL-Hor De Bilt (NL) / Loenen aan de Vecht (NL)	0.50/1.24/0.96	0.50/1.36/1.05

**Table 4.** Pearson correlation coefficients, RMSE (in [mm/day]) and rRMSE values between  $ET_a$  data from selected FluxNet stations and simulated  $ET_a$  values from SWAP and SoilClim. Each row has a line added with the nearest meteorological station (providing temperature and global radiation) and the nearest rain gauge respectively.

The depth levels for which soil moisture is provided is not standardized in the ISMN repository. Motivated by this, we  
 355 matched the calculated soil moisture levels at the surface and rootzone levels from SWAP and SoilClim to a range of levels  
 which were provided by the selected ISMN stations. Measured soil moisture at the upper 10 cm in the soils (and in a few cases  
 in the upper 20 cm) are compared against the calculated surface soil moisture. When observations are available until a depth of  
 50 cm, then these are related to the root zone.

Table A1 shows the correlation, RMSE and rRMSE values of the comparison of observed soil moisture values at surface,  
 360 rootzone and deep levels from the ISMN stations with the simulations of SWAP and SoilClim forced by the observations  
 from the nearest ECA&D station. The general picture that emerges from this table is that correlations between modelled and  
 observed soil moisture are on average around 0.55. For the surface layer, the average correlations between the ISMN series and  
 the SWAP or SoilClim output are 0.55 and 0.52 respectively. For the root zone, these numbers are 0.51 and 0.64 for SWAP  
 and SoilClim respectively. When the correlation is poor between ISMN observed soil moisture and a model, it will be poor  
 365 for the other model as well. This suggests that for the poorly correlating stations, the selection of the nearest meteorological

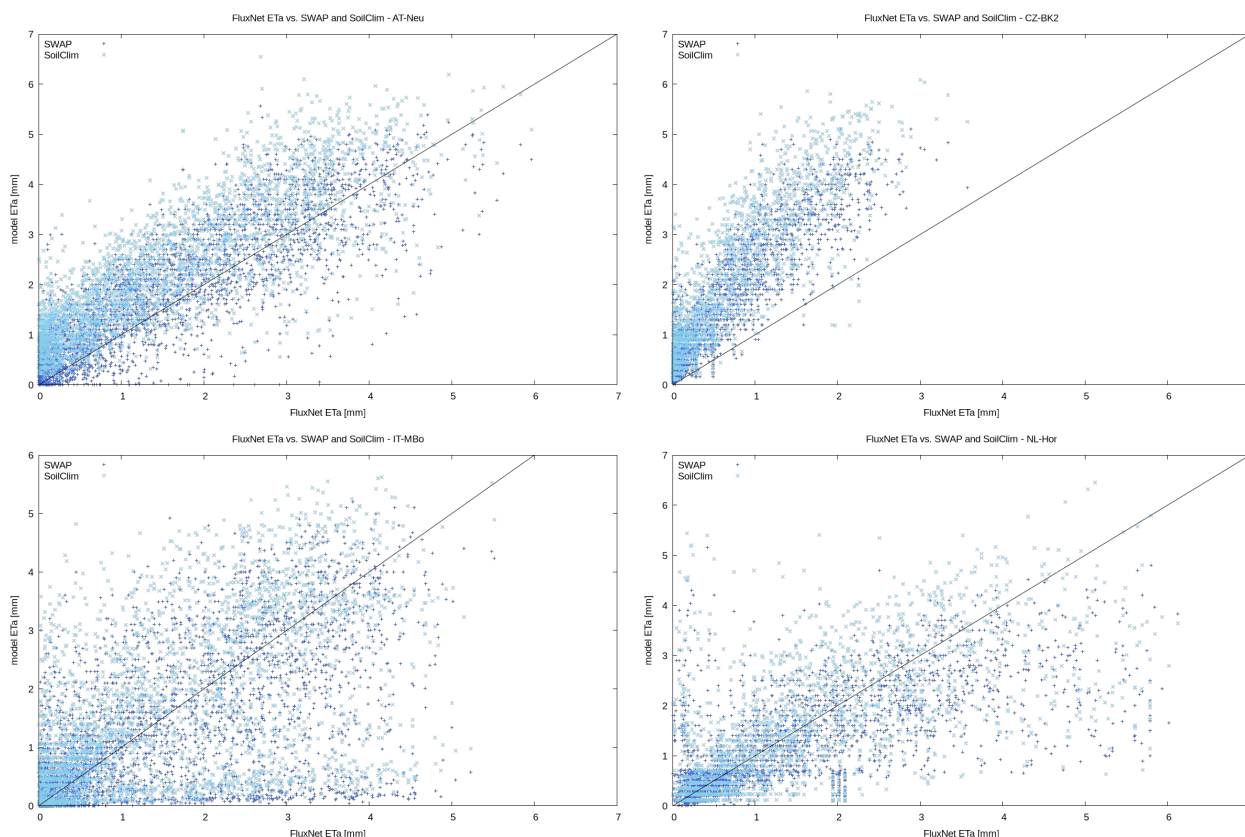


**Figure 5.** Scatterplots with observed  $ET_a$  values from the FluxNet station on the horizontal axis and modelled  $ET_a$  values from SWAP (dark blue) and SoilClim (light blue), for FluxNet stations AT-Neu, CZ-BK2, IT-MBo and NL-Hor.

station is not optimal. For the surface and root-zone layers, the SWAP model has a consistently lower rRMSE than SoilClim which mirrors the observation from the comparison with  $ET_a$  of the FluxNet stations that SWAP models the vertical motion of moisture in and out of the soil more realistically. However, for the deep layer, the SoilClim model has a lower rRMSE.

Figure 7 shows examples from ISMN stations San Pietro Capofiume, Hoal\_01 and Berzeme showing scatter diagrams between observed ISMN values and modelled SWAP and SoilClim values for the surface layer and root zone. The clustering of point at the top-end of the diagrams shows that the SoilClim model tends to saturate earlier than what is observed and what is modelled by SWAP. For the Berzeme station, the SoilClim shows a quicker depletion of soil water from the surface layer.

The average seasonal cycle in soil water content for the rootzone is shown in fig. 8. For station San Pietro Capofiume, the two models simulations agree fairly well but the saturation in soil moisture in late winter and early spring by SoilClim is obvious. Both models show a stronger depletion in soil moisture in summer than the observations. For station Hoal\_01, the medians in the seasonal cycles are not too far apart - except for SoilClim's saturation in late winter, early spring and a decrease in SWAP's soil moisture for mid-spring. The resemblance in seasonal cycle for station Berzeme between observations and model results

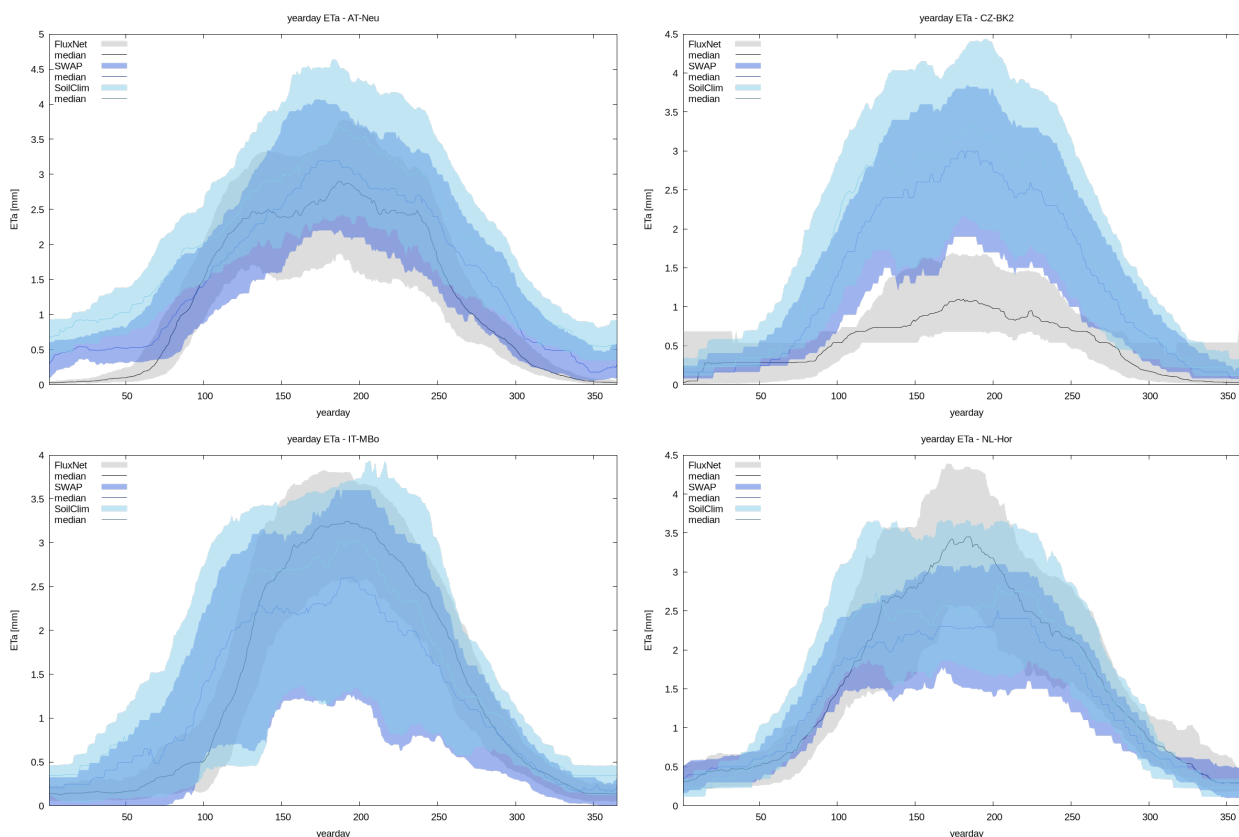


**Figure 6.** Comparison of the average seasonal cycle of  $ET_a$  as provided by the observation (gray), SWAP (dark blue) and SoilClim (light blue), for FluxNet stations AT-Neu, CZ-BK2, IT-MBo and NL-Hor. The lines represent the median values and the shaded areas give the range between the 25<sup>th</sup> and 75<sup>th</sup> percentiles.

is clearly the worst of the subset shown in this figure. While the model results agree fairly well, they overestimate the observed soil water content.

## 380 5 Climate Assessment

### 5.1 The historical perspective

The length of the records in ECA&D allows for putting recent extreme events into a fairly long historical perspective without losing the pan-European scope. An example is the relatively recent drought of 2018 which is often compared in terms of severity with the drought of 1976. Figure 9 shows the number of moisture stressed days (SMIO) in summer for both these  
385 years. It shows that for both years the epicentre of the drought was in central Europe with the complete season experiencing moisture stress. But the 1976 drought had a larger extent to the west, over the Netherlands into England, to the south-west over

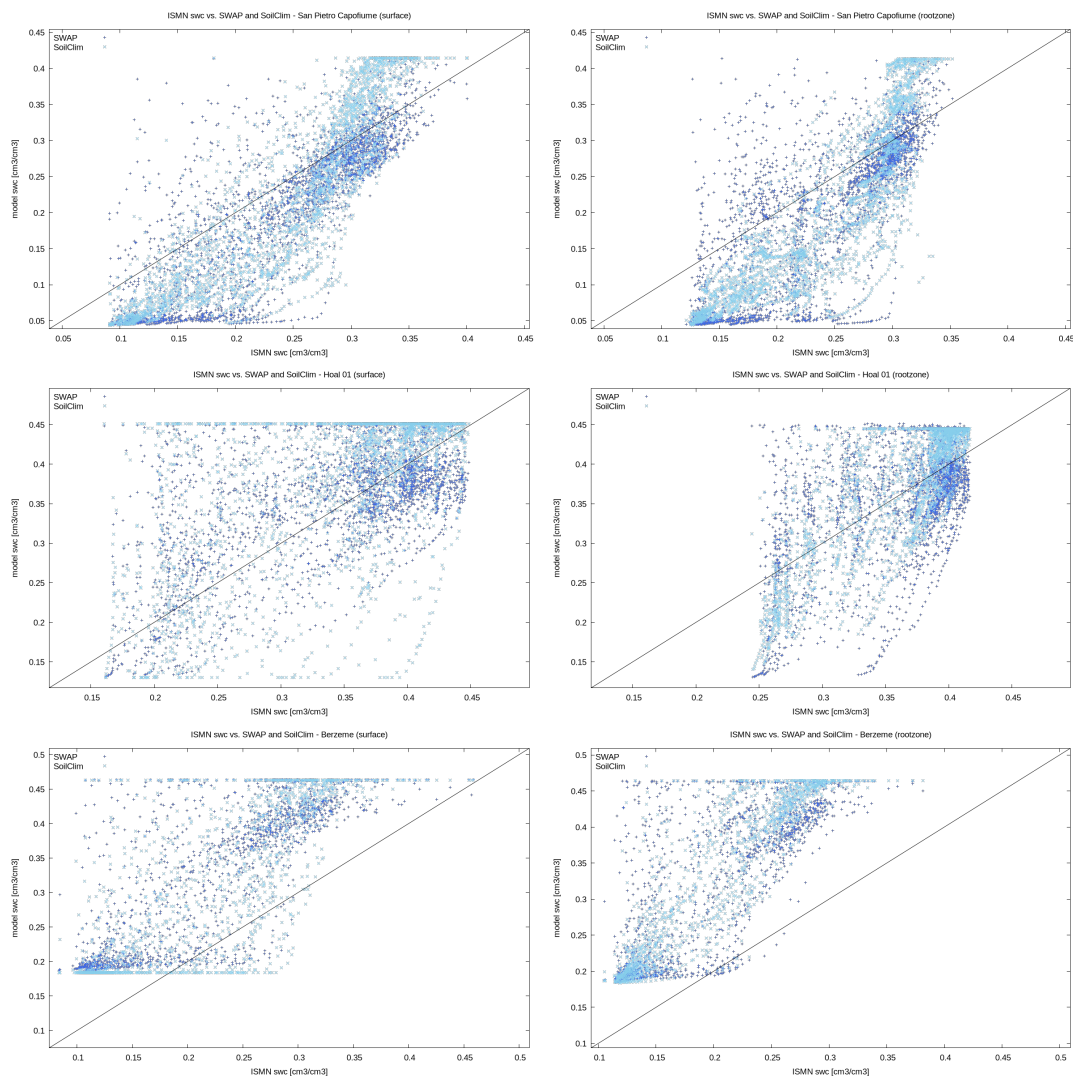


**Figure 7.** Scatter plots with observed soil moisture from ISMN on the horizontal axis and modelled soil moisture values from SWAP (dark blue) and SoilClim (light blue) for the surface and rootzone. Top row shows station ISMN station San Pietro Capofiume, the middle row shows ISMN station Hoal\_01 and the bottom row shows results for ISMN station Berzeme.

France and into Spain, to the north into southern Scandinavia and to the east over Poland. Similar maps for spring (not shown) show that spring 1976 was already much drier in terms of the number of days with moisture stress than 2018. Similar to 1921, Europe's worst drought event, the conservative nature of soil moisture causes that the lack of precipitation in spring is carried forward into the following summer, amplifying summer drought (van der Schrier et al., 2021).

Drought monitoring is of immediate relevance in a soil moisture dataset, but for agriculture excessive wet conditions in the soils can be equally problematic, as this may yield root rot, fungal infections or enhanced pest pressure, stunted growth or

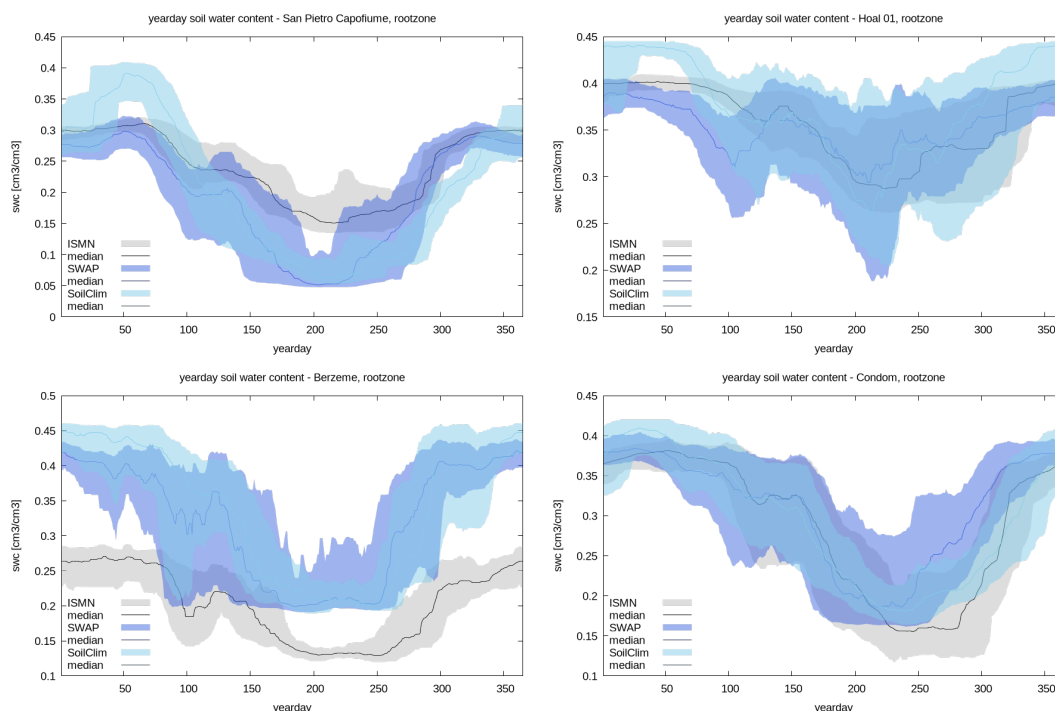


**Figure 8.** Comparison of the average seasonal cycle of soil water content in the rootzone as provided by the observation (gray), SWAP (dark blue) and SoilClim (light blue), for ISMN stations San Pietro Capofiume, Hoal\_01, Berzeme and Condom. The lines represent the median values and the shaded areas give the range between the 25<sup>th</sup> and 75<sup>th</sup> percentiles.

reduced germination. Soils that are too wet are impossible to access, disrupting the harvesting schedule (Wigley and Atkinson, 1977). A recent example of a very wet spring was 2024 in western Europe (C3S, 2024). Figure 10 (upper panel) shows the number of very moisture saturated days in De Bilt and Brno in spring. It shows that 2024 is indeed high, but ranks third since 1961 (after 1983 and 1977). This figure also shows that such moisture saturated days in spring are rare in Brno.

This contrasts with a time series of very moisture stressed days (AW10p). Figure 10 (lower panel) shows that most of the springs in Brno, and nearly all in De Bilt, lack such very dry situations. However, the recent decades in Brno show an increase in springs with very moisture stressed days, although none reach the level of the 1974 spring. In the period since 1960, De Bilt experienced 10 very moisture stressed days in the 2002 spring.

## 5.2 First assessment of climatology and trends

In an interesting 20-year old publication, Robock et al. (2005) analysed 141 soil moisture records from the Ukraine spanning the period from 1958 to 2002. In that publication, no summer desiccation was (yet) found which was the initial hypothesis given that the climate projections available at the time indicated gradually more droughty summer conditions. Instead the observations indicated an overall positive (wetting) trend over this period with the trend leveling off in the last two decades of

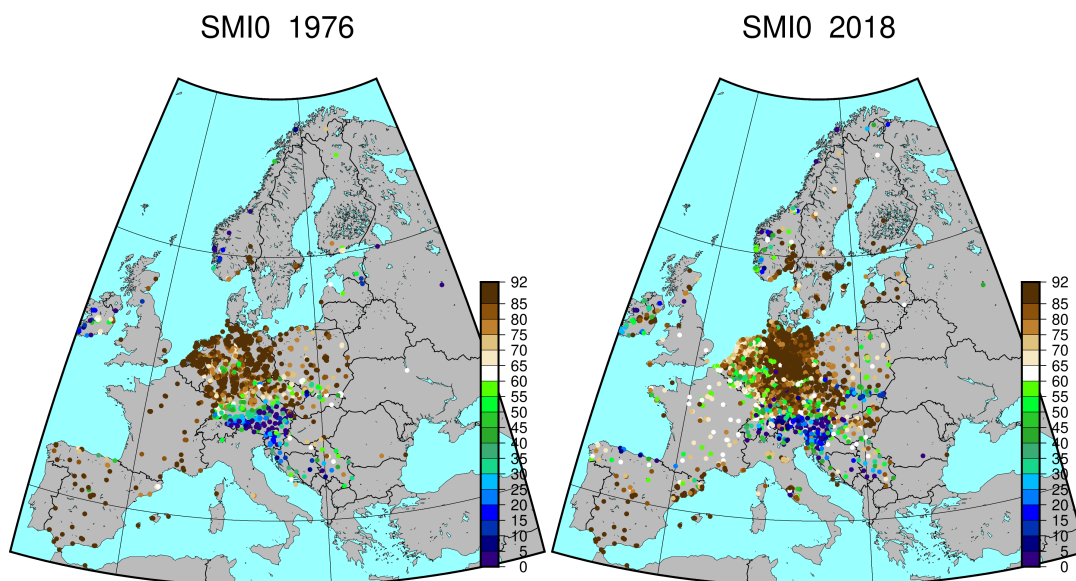


**Figure 9.** Comparison of the SMI0 index for summer 1976 (left) and 2018 (right) which were both very dry summers in NW Europe.

the period they observed. In this section, a first brief look at the climatology of the four proposed indices is taken and an initial trend analysis is made to assess if summer desiccation is observed over Europe.

Figure 11 shows the spring and summer 1991-2020 climatology of the indices SMI and SMI0. The climatological SMI spring values are without exception positive, meaning that for an average spring and on average over the season, moisture stress will not be an issue. It is interesting that in Ireland, Norway and northern Scandinavia the SMI values are relatively close to zero. In summer, this picture changes considerably. The areas that remain (for an average summer and on average over the season) free of moisture stress are Scandinavia, Ireland and northern UK, the low countries, the greater Alpine area and the Caucasus. A clear gradient to the south-west into Spain and into the east toward Poland of more severe moisture stress is seen.

The spring climatology of the number of days with moisture stress (SMI0) shows that no or hardly any days are observed for much of the domain, but Spain, southern France, the Balkan and Poland show areas where already a significant number of days fall below the SMI=0 threshold. For summer, the area with a large number of days experiencing moisture stress is quite large and only the highest parts of the Alps, Ireland, the northern UK and Norway have a more modest number of moisture stress days.

Figure 12 shows the trends over the spring and summer season in the period 1979-2023 for the number of moisture stress days (SMI0) and the Soil Moisture Index (SMI) for spring and summer respectively. The trends are calculated using the Theil-Sen regression and the significance of the trend is determined from the Mann-Kendall test. The trends that pass the 95% significance level are plotted as black-rimmed circles. The trend map for spring SMI0 generally shows an increase in the number of moisture stressed days over Europe, with the strongest trends in northern Spain, France, Central Europe and

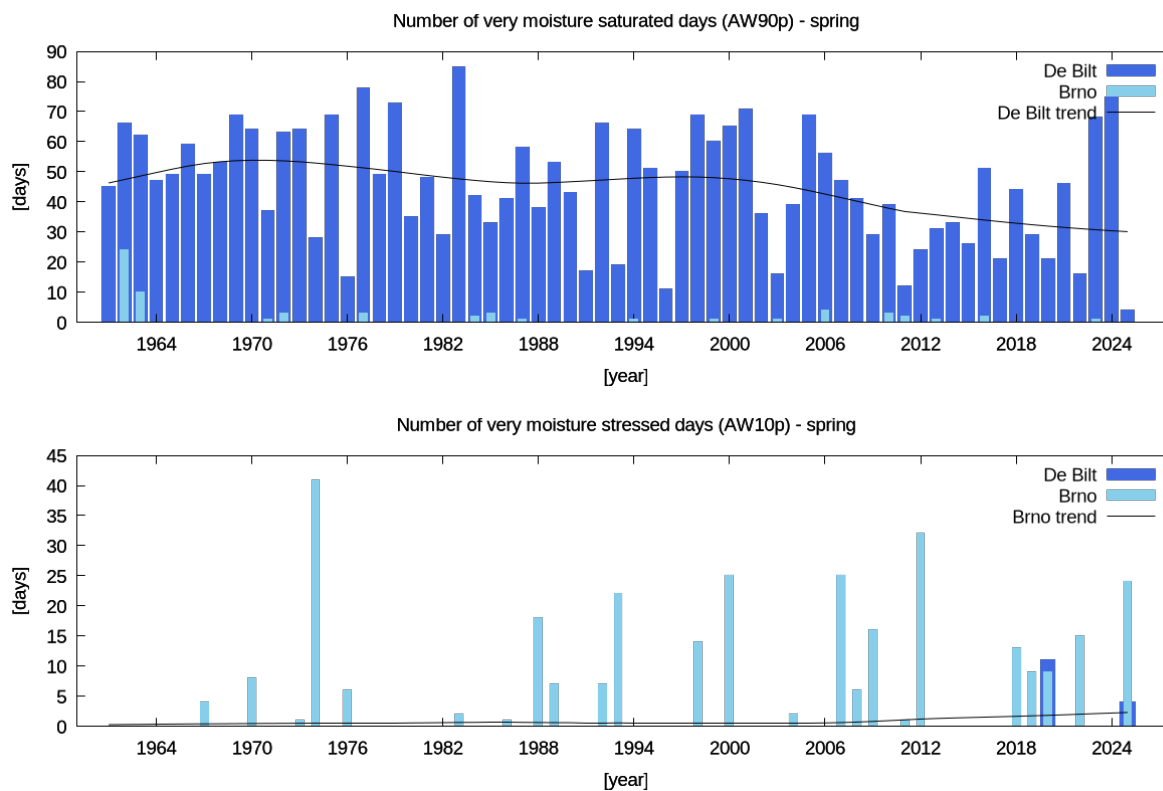


**Figure 10.** Time series for the number of number of very moisture saturated days (AW90p) and the very moisture stressed days (AW10p) in spring, for stations De Bilt , the Netherlands and Brno, Czech Republic.

425 southern Scandinavia. In eastern Poland and the Slovak Republic and central Balkan peninsula, a decrease in the number of  
moisture stressed days is observed. Figure 12 shows a slight wetting trend of SMI summer values in Ireland, Scandinavia, a  
few stations along the North Sea coast and some scattered station in Central Europe. Most of the stations in Spain, France,  
Central Europe and southern Sweden show a trend toward drying. It would be interesting to analyse these results to determine  
430 if the observed increase in solar radiation over Europe for spring could be related to this trend (Sanchez-Lorenzo et al., 2015;  
Hodnebrog et al., 2024). It is interesting to revisit the conclusions of Robock et al. (2005) and put their observation in a more  
recent perspective. Although the trend maps of this study do not show results over the Ukraine (because of a lack of data), the  
results in Figure 12b indicate that the anticipated decrease in soil moisture is now widely visible across Europe.

## 6 Discussion and conclusions

The research on the soil moisture - climate interactions has accelerated in past few decades. This is strongly fuelled by the  
435 observed relation between soil moisture, evapotranspiration and air temperature (e.g. Seneviratne et al. (2006); Teuling et al.

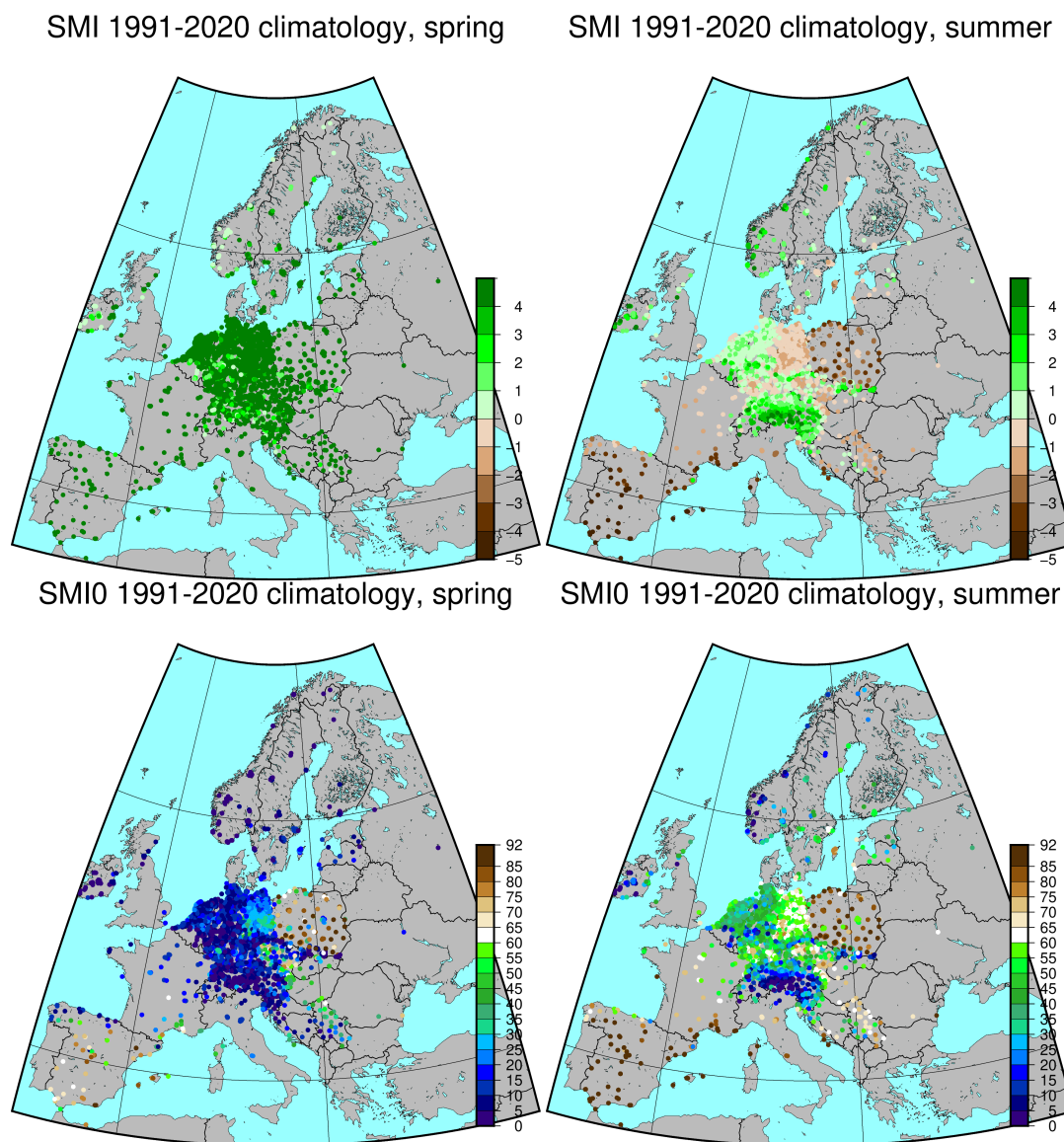


**Figure 11.** Climatological values over the 1991-2020 period for SMI (upper row) and SMI0 (bottom row), for spring (left) and summer (right).

(2010, 2013)). This relation emphasizes the importance of soil-moisture–temperature feedbacks in influencing spring and summer climate variability. An example where hot extremes and droughty conditions go hand-in-hand is the latest WMO RA VI Europe (continental) heat extreme of 48.8°C in Siracusa Sicilia, Italy on August 11, 2021 (Merlone et al., 2024). In the temperate climate zone, prolongation of the growing season and shortening of the period with snow cover and frozen soil is

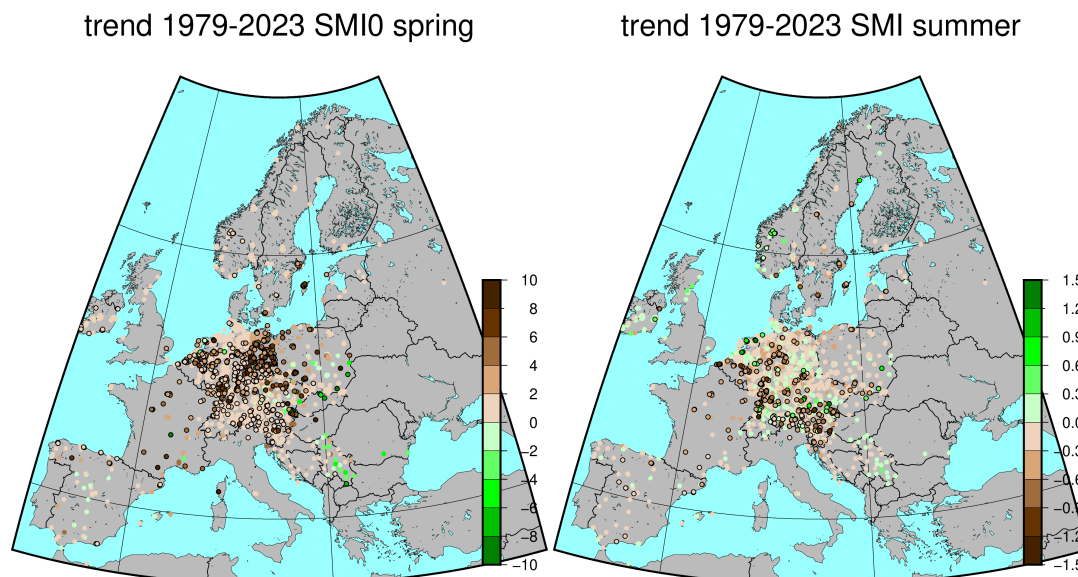


**Figure 12.** Trends over the 1979-2023 period for spring SMI0 (left) and summer SMI (right). The unit of the trends is index/decade for SMI and days/decade for SMI0. Trends that reach the 95% significance level are plotted with a black rimmed circle.

440 causing earlier soil moisture decrease during spring with a higher probability of early soil moisture deficit, which is another  
example of an important soil moisture - temperature feedback (Ionita et al., 2017; Řehoř et al., 2024).

In the dataset presented here, the challenge put forward by Seneviratne et al. (2010) to optimize the use of existing observed  
information for soil moisture - climate research is taken up. A pan-European dataset with *in situ* observations of meteorological  
parameters (ECA&D) is used to calculate daily soil moisture values for the surface and the rootzone, using a state-of-the art  
445 soil dynamics model. This has resulted in a dataset of nearly 6000 stations (status July 2025) for which a set of four climate  
impact indices is calculated for monitoring purposes. The aim is to update the dataset regularly along with the regular updates  
of ECA&D. However, the bottleneck of the current set-up are the lack of *in situ* global radiation and/or sunshine duration data.  
With over 20,000 rain gauges in the dataset, there is some potential to increase the coverage in some places and make the  
coverage denser in others. Increasing the number of long-running sunshine duration records - there are now about 400 stations  
450 that provide sunshine duration data back to 1950 provides the potential to extend the historical perspective further back in time.

An important motivation to focus on short-term variations in soil water content is the recent insight that flash droughts are  
more common than previously thought - also in Europe (Shah et al., 2022; Yuan et al., 2023). Flash droughts are a recently  
recognized type of extreme event distinguished by sudden onset and rapid intensification of drought conditions with severe  
impacts (Lesinger and Tian, 2022). They unfold on sub-seasonal-to-seasonal timescales (weeks to months) (Pendergrass et al.,  
455 2023; Yuan et al., 2023) and can develop into severe droughts in a few weeks. In addition to precipitation deficits, flash droughts  
are also caused by abnormally high evapotranspiration that rapidly depletes the soil water. The intermittent nature and rapid



onset of such droughts challenge existing drought monitoring capabilities and point to the necessity of having an active role of evapotranspiration in drought monitoring and the focus on short - like daily - time scales.

460 The approach taken here to provide calculated soil moisture is not new, Cammalleri et al. (2016) used the E-OBS gridded observational data (Haylock et al., 2008; Cornes et al., 2018) as meteorological forcing for the LISFLOOD model. The same model is the basis for the European Drought Observatory of the EU's Copernicus Emergency Management Service as part of a near-real-time drought monitoring (Cammalleri et al., 2021) using meteorological station data as input. Earlier, Orth and Seneviratne (2015) used the E-OBS data in combination with a simple water balance model to provide a hydrological dataset covering a few decades. This dataset was subsequently used by Whan et al. (2015) to study the impact of soil moisture on  
465 temperature extremes. Note that the gridded E-OBS dataset is based on the station data of ECA&D which is the dataset used in this study.

In conclusion, the soil water content dataset presented here aims to provide a wide network of stations for which an estimate of soil water content in the surface and rootzone is provided. These data are based on observed meteorological input data that are provided by the European NMHSs and are arguably soil moisture data that are closest to actual observed soil moisture data.

470 *Data availability.* Data described in this manuscript can be accessed at the KNMI Data Platform (<https://datapatform.knmi.nl>) under data DOI:10.21944/phk8-at71 (van der Schrier et al., 2026). The time series with soil water content for the upper 10 cm and for the upper 40 cm of the soils as calculated by the SoilClim model with input of observed meteorological data are also available at the European Climate Assessment & Dataset, <https://www.ecad.eu>. These data can be accessed either as bulk download or a selection can be made through a download form. The climate indices data are accessible through his data portal as well, both in bulk download and through more specified  
475 queries.



## Appendix A: Comparisons against the ISMN stations

name	period	surface layer		root zone layer	
		SWAP	SoilClim	SWAP	SoilClim
Banloc	20141120-20220531	0.46/2.88/18.94	0.17/3.77/24.80	-/-	-/-
Dumbraveni	20140611-20210527	0.25/0.20/1.37	0.27/0.22/1.46	-/-	-/-
Berzeme	20081114-20201228	0.78/0.12/0.54	0.75/0.12/0.52	0.74/0.14/0.68	0.89/0.14/0.69
Mouthoumet	20070101-20181210	0.68/0.12/0.51	0.67/0.11/0.48	0.65/0.12/0.53	0.77/0.10/0.43
P2	20080222-20130506	0.02/0.51/0.60	0.13/0.48/0.56	-0.02/0.54/0.61	0.09/0.52/0.58
Tambovskaya #1	20080222-20130506	0.61/0.10/0.24	0.57/0.11/0.27	-/-	-/-
Rodnikovka	19780218-19851028	0.56/0.08/0.29	0.52/0.08/0.27	-/-	-/-
Semikarakorsk	19780128-19851228	0.64/0.11/0.57	0.63/0.11/0.58	-/-	-/-
Terekty	19780218-19851028	0.65/0.12/0.71	0.45/0.10/0.55	-/-	-/-
Uralsk	19780328-19851108	0.57/0.11/0.45	0.54/0.09/0.35	-/-	-/-
ParcMeteo	20120101-20220101	0.59/0.23/1.77	0.62/0.22/1.69	0.52/0.23/1.69	0.71/0.22/1.61
1.06	20120101-20220101	-/-	-/-	0.58/0.29/1.54	0.72/0.28/1.50
Satu Mare	20140723-20220531	0.32/0.22/1.61	0.21/0.23/1.66	-/-	-/-
Creon d' Armagnac	20070107-20171011	0.66/0.20/1.25	0.71/0.19/1.21	0.61/0.21/1.51	0.84/0.21/1.46
CAN_CT_NT	20151204-20220209	0.56/0.10/0.42	0.46/0.11/0.48	0.65/0.09/0.28	0.78/0.07/0.23
Colorso	20021009-20080531	-/-	-/-	0.66/0.11/0.40	0.71/0.11/0.43
Torre Olmo	20100919-20171231	-/-	-/-	0.52/0.12/0.46	0.60/0.12/0.47
27	20131023-2022050	-/-	-/-	0.43/0.10/0.25	0.66/0.09/0.22
Belgorodskaya #1	19700408-19980818	0.61/0.09/0.35	0.48/0.13/0.47	-/-	-/-
Chuvashskaya Republic #2	19700418-19981028	0.44/0.14/0.51	0.42/0.14/0.50	-/-	-/-
Kalmkskaya #2	19870508-19981008	0.50/0.09/0.38	0.42/0.10/0.43	-/-	-/-
Krasnodarskaya #1	19920418-19970628	0.48/0.16/0.40	0.49/0.16/0.40	-/-	-/-
Kurskaya #1	19700418-19980728	0.61/0.09/0.30	0.51/0.11/0.36	-/-	-/-
Lipetskaya #1	19700418-19980808	0.42/0.09/0.23	0.32/0.10/0.26	-/-	-/-
Peyrusse Grande	20070107-20210101	0.78/2.79/9.40	0.65/2.87/9.67	0.80/11.53/38.77	0.77/11.97/40.26
Merzenhausen	20111103-20200805	-/-	-/-	-0.04/945.43/6.23	-0.12/945.44/6.23
Neusling	20071108-20111118	0.42/0.07/0.20	0.41/0.07/0.21	0.43/0.10/0.39	0.31/0.11/0.45
San Pietro Capofiume	20090612-20170515	0.84/0.06/0.27	0.87/0.07/0.29	0.74/0.08/0.32	0.86/0.08/0.32
Gruzia #1	19920508-19980628	-0.03/0.11/0.52	0.11/0.10/0.44	-/-	-/-
Lipetskaya #2	19700408-19981108	0.52/0.08/0.19	0.63/0.06/0.15	-/-	-/-
Mordovskaya Republic #1	19700418-19980728	0.43/0.12/0.46	0.65/0.12/0.46	-/-	-/-
Rostovskaya #1	19700418-19980708	0.71/0.08/0.23	0.77/0.07/0.18	-/-	-/-
Ulyanovskaya #2	19700428-19981028	0.47/0.12/0.48	0.68/0.10/0.39	-/-	-/-
Phrolovo	19780218-19851108	0.71/0.14/0.65	0.72/0.13/0.60	-/-	-/-
Tsyvilk	19780128-19851118	0.44/0.24/1.08	0.76/0.22/1.01	-/-	-/-

**Table A1.** ISMN station name, start & stop dates and the Pearson correlation, the RMSE and rRMSE values respectively with SWAP and SoilClim for the surface and the root zone.



name	period	surface SWAP	surface SoilClim	root zone SWAP	root zone SoilClim
Mari Republic #1	19700428-19980728	0.31/0.18/0.70	0.28/0.18/0.70	-/-	-/-
Mordovskaya Republic #2	19700418-19981008	0.62/0.09/0.33	0.56/0.11/0.38	-/-	-/-
Orlovskaya #1	19700408-19980908	0.45/0.11/0.32	0.42/0.12/0.35	-/-	-/-
Penzenskaya #2	19700418-19981108	0.61/0.09/0.23	0.57/0.11/0.27	-/-	-/-
Severo-Osetinskaya Republic	19920508-19981028	0.51/0.10/0.42	0.29/0.13/0.53	-/-	-/-
Smolenskaya #2	19700428-19981028	0.39/0.15/0.48	0.48/0.15/0.48	-/-	-/-
Stavropolskaya #1	19700408-19980718	0.41/0.14/0.38	0.30/0.16/0.43	-/-	-/-
Tatar Republic #1	19700508-19980828	0.44/0.09/0.22	0.40/0.10/0.25	-/-	-/-
Tulskaya #2	19700418-19981108	0.38/0.13/0.39	0.38/0.13/0.39	-/-	-/-
Voronezhskaya #1	19700408-19980818	0.55/0.11/0.43	0.45/0.12/0.46	-/-	-/-
Yaroslavl'skaya #2	19700408-19980818	0.43/0.17/0.56	0.50/0.17/0.55	-/-	-/-
Aglos	19780128-19851028	0.65/0.14/0.55	0.68/0.15/0.60	-/-	-/-
Ershov	19780128-19851228	0.63/0.13/0.60	0.59/0.14/0.65	-/-	-/-
Gigant	19780128-19851228	0.76/0.12/0.32	0.62/0.15/0.40	-/-	-/-
Izhevsk	19780128-19821228	0.56/0.18/0.60	0.58/0.17/0.57	-/-	-/-
Kamyshevatskaya	19780218-19851208	0.65/0.14/0.37	0.58/0.16/0.42	-/-	-/-
Rostoshy	19780218-19851208	0.64/0.10/0.28	0.60/0.10/0.30	-/-	-/-
Tchebenki	19780218-19851208	0.73/0.11/0.42	0.67/0.10/0.41	-/-	-/-
Tchishmy	19780218-19851208	0.61/0.08/0.19	0.58/0.09/0.22	-/-	-/-
Hoal 01	20130820-20201231	0.60/0.07/0.20	0.59/0.08/0.25	0.52/0.06/0.17	0.82/0.05/0.14
Falkenberg	20030101-20200630	-/-	-/-	0.47/0.22/1.35	0.84/0.19/1.17
Chevru	20080227-20130822	0.79/0.25/96.67	0.76/0.32/123.14	-/-	-/-
Esternay	20080523-20130904	0.75/0.26/94.21	0.70/0.32/115.70	-/-	-/-
Suizy	20060719-20130905	0.60/0.11/0.33	0.56/0.11/0.33	0.48/0.11/0.34	0.60/0.10/0.31
Voulton	20060808-20130905	0.45/0.20/0.48	0.43/0.17/0.42	0.40/0.16/0.40	0.52/0.12/0.31
La Atalaya	20050316-20171211	0.52/0.23/2.04	0.44/0.21/1.79	-/-	-/-
Las Arenas	20050322-20220101	0.62/0.19/1.12	0.58/0.16/0.95	-/-	-/-
Condom	20070107-20190214	0.74/0.06/0.18	0.72/0.07/0.23	0.66/0.08/0.29	0.84/0.06/0.20
Montaut	20070107-20170727	0.55/0.08/0.28	0.55/0.09/0.30	0.49/0.11/0.44	0.61/0.10/0.41

**Table A1.** Continued



*Author contributions.* GvdS: Conceptualization, Validation, Formal Analysis, Investigation, Writing- Original draft preparation. MF: Conceptualization, Software, Writing- Reviewing and Editing. MM: Software, Writing- Reviewing and Editing. JvD: Software, Writing- Reviewing and Editing. JR: Software, Formal Analysis, Writing- Reviewing and Editing. MT: Conceptualization, Writing- Reviewing and  
480 Editing,

*Competing interests.* The authors declare that no competing interests are present.

*Acknowledgements.* GvdS, MF and MT received support from SustES—Adaptation strategies for sustainable ecosystem services and food security under adverse environmental conditions (CZ.02.1.01/0.0/0.0/16\_019/0000797). Data providers in the ECA&D project are acknowl-  
485 edged (<https://www.ecad.eu>).



## References

- Allen, R. G., Smith, M., Perrier, A., and Pereira, L. S.: An update for the calculation of reference evapotranspiration, *ICID Bulletin*, 43, 35–92, 1994.
- Allen, R. G., Pereira, L. S., Raes, D., and Smith, M.: Crop evapotranspiration - Guidelines for computing crop water requirements, Tech. Rep. FAO Irrigation and drainage paper 56, Food and Agriculture Organization of the United Nations, Rome, 1998.
- 490 Ardilouze, C., Materia, S., Batté, L., Benassi, M., and Prodhomme, C.: Precipitation response to extreme soil moisture conditions over the Mediterranean, *Climate Dyn.*, 58, 1927–1942, <https://doi.org/10.1007/s00382-020-05519-5>, 2022.
- Barker, D., Beuerlein, J., Dorrance, A., Eckert, D., Eisley, B., Hammond, R., Lentz, E., Lipps, P., Loux, M., Mullen, R., Sulc, M., Thomison, P., and Watson, M.: Ohio Agronomy Guide 14th edition, vol. 472, Ohio State University Extension, accessed: 2024-08-08, 2005.
- 495 Betts, A. K.: Understanding hydrometeorology using global models, *Bull. Amer. Meteor. Soc.*, 85, 1673–1688, 2004.
- Bontemps, S., Defourny, P., Radoux, J., Van Bogaert, E., Lamarche, C., Achard, F., Mayaux, P., Boettcher, M., Brockmann, C., Kirches, G., et al.: Consistent global land cover maps for climate modelling communities: current achievements of the ESA's land cover CCI, in: *Proceedings of the ESA living planet symposium, Edinburgh*, vol. 13, pp. 9–13, 2013.
- C3S: European State of the Climate - European wet and dry conditions, <https://climate.copernicus.eu/ESOTC/2019/european-wet-and-dry-conditions>, 2020.
- 500 C3S: European State of the Climate, <https://doi.org/10.24381/14j9-s541>, 2024.
- Cammalleri, C., Micale, F., and Vogt, J.: Recent temporal trend in modelled soil water deficit over Europe driven by meteorological observations, *Int. J. Climatol.*, 36, 4903–4912, doi:10.1002/joc.4677, 2016.
- Cammalleri, C., Arias-Muñoz, C., Barbosa, P., de Jager, A., Magni, D., Masante, D., Mazzeschi, M., McCormick, N., Naumann, G., Spinoni, J., and Vogt, J.: A revision of the Combined Drought Indicator (CDI) used in the European Drought Observatory (EDO), *Natural Hazards and Earth System Sciences*, 21, 481–495, <https://doi.org/10.5194/nhess-21-481-2021>, 2021.
- 505 Cavanaugh, N. R., Gershunov, A., Panorska, A. K., and Kozubowski, T. J.: The probability distribution of intense daily precipitation, *Geophys. Res. Lett.*, 42, 1560–1567, doi:10.1002/2015GL063238, 2015.
- Cornes, R. C., van der Schrier, G., van den Besselaar, E. J. M., and Jones, P. D.: An Ensemble Version of the E-OBS Temperature and Precipitation Datasets, *J. Geophys. Res. (Atmospheres)*, 123, 9391–9409, doi:10.1029/2017JD028200, 2018.
- 510 de Bruin, H. A. R.: The determination of (reference crop) evapotranspiration from routine weather data, in: *Evaporation in relation to Hydrology*, edited by Hooghardt, C., Proceedings and Informations 28, pp. 5–31, Commission for Hydrological Research TNO, The Hague, the Netherlands, 1981.
- de Bruin, H. A. R.: From Penman to Makkink, in: *Evaporation and Weather*, edited by Hooghardt, C., Proceedings and Informations 39, pp. 5–31, Commission for Hydrological Research TNO, The Hague, the Netherlands, 1987.
- 515 de Bruin, H. A. R. and Holtslag, A. A. M.: A Simple Parameterization of the Surface Fluxes of Sensible and Latent Heat During Daytime Compared with the Penman-Monteith Concept, *J. Appl. Meteor.*, 21, 1610–1621, 1982.
- de Bruin, H. A. R. and Stricker, J. N. M.: Evaporation of grass under non-restricted soil moisture conditions, *Hydrological Sciences*, 45, 391–406, 2000.
- 520 Dorigo, W., Wagner, W., Hohensinn, R., Hahn, S., Paulik, C., Xaver, A., Gruber, A., Drusch, M., Mecklenburg, S., Oevelen, P. v., Robock, A., and Jackson, T.: The International Soil Moisture Network: a data hosting facility for global in situ soil moisture measurements, *Hydrology and Earth System Sciences*, 15, 1675–1698, <https://doi.org/10.5194/hess-15-1675-2011>, 2011.



- 525 Dorigo, W., Preimesberger, W., Reimer, C. Van der Schalie, R., Pasik, A., De Jeu, R., and Paulik, C.: Soil moisture gridded data from 1978 to present, v201912.0.0. Copernicus Climate Change Service (C3S) Climate Data Store (CDS), <https://cds.climate.copernicus.eu/cdsapp#!/dataset/satellite-soil-moisture?tab=overview>, 2019.
- 530 Dorigo, W., Himmelbauer, I., Aberer, D., Schremmer, L., Petrakovic, I., Zappa, L., Preimesberger, W., Xaver, A., Annor, F., Ardö, J., Baldocchi, D., Bitelli, M., Blöschl, G., Boga, H., Brocca, L., Calvet, J.-C., Camarero, J. J., Capello, G., Choi, M., Cosh, M. C., van de Giesen, N., Hajdu, I., Ikonen, J., Jensen, K. H., Kanniah, K. D., de Kat, I., Kirchengast, G., Kumar Rai, P., Kyrouac, J., Larson, K., Liu, S., Loew, A., Moghaddam, M., Martínez Fernández, J., Mattar Bader, C., Morbidelli, R., Musial, J. P., Osenga, E., Palecki, M. A., Pellarin, T., Petropoulos, G. P., Pfeil, I., Powers, J., Robock, A., Rüdiger, C., Rummel, U., Strobel, M., Su, Z., Sullivan, R., Tagesson, T., Varlagin, A., Vreugdenhil, M., Walker, J., Wen, J., Wenger, F., Wigneron, J. P., Woods, M., Yang, K., Zeng, Y., Zhang, X., Zreda, M., Dietrich, S., Gruber, A., van Oevelen, P., Wagner, W., Scipal, K., Drusch, M., and Sabia, R.: The International Soil Moisture Network: serving Earth system science for over a decade, *Hydrol. Earth Syst. Sci.*, 25, 5749–5804, <https://doi.org/10.5194/hess-25-5749-2021>, 2021.
- 535 Driemel, A., Augustine, J., Behrens, K., Colle, S., Cox, C., Cuevas-Agulló, E., Denn, F. M., Duprat, T., Fukuda, M., Grobe, H., et al.: Baseline Surface Radiation Network (BSRN): structure and data description (1992–2017), *Earth System Science Data*, 10, 1491–1501, 2018.
- ECA&D Project Team: European Climate Assessment & Dataset Algorithm Theoretical Basis Document (ATBD), De Bilt, NL, version 10.5, 2012.
- ESA: ESA Land Cover CCI – User Requirements Document (URD), Tech. rep., European Space Agency, available online at [https://climate.esa.int/media/documents/Land\\_Cover\\_CCI\\_URD\\_2.2.pdf](https://climate.esa.int/media/documents/Land_Cover_CCI_URD_2.2.pdf), 2011.
- 540 EU Commission: EU Regulation 2023/138, [https://eur-lex.europa.eu/eli/reg\\_impl/2023/138/oj](https://eur-lex.europa.eu/eli/reg_impl/2023/138/oj), 2022.
- Fan, Y., Li, H., and Miguez-Macho, G.: Global patterns of groundwater table depth, *Science*, 339, 940–943, <https://doi.org/10.1126/science.1229881>, 2013.
- 545 Graf, A., Klosterhalfen, A., Arriga, N., Bernhofer, C., Boga, H., Bornet, F., Brüggemann, N., Brümmer, C., Buchmann, N., Chi, J., Chipeaux, C., Cremonese, E., Cuntz, M., Dušek, J., El-Madany, T. S., Fares, S., Fischer, M., Foltýnová, L., Gharun, M., Ghiasi, S., Gielen, B., Gottschalk, P., Grünwald, T., Heinemann, G., Heinesch, B., Heliasz, M., Holst, J., Hörtnagl, L., Ibrom, A., Ingwersen, J., Jurasinski, G., Klatt, J., Knohl, A., Koebsch, F., Konopka, J., Korkiakoski, M., Kowalska, N., Kremer, P., Kruijt, B., Lafont, S., Léonard, J., De Ligne, A., Longdoz, B., Loustau, D., Magliulo, V., Mammarella, I., Manca, G., Mauder, M., Migliavacca, M., Mölder, M., Neiryneck, J., Ney, P., Nilsson, M., Paul-Limoges, E., Peichl, M., Pitacco, A., Poyda, A., Reibmann, C., Roland, M., Sachs, T., Schmidt, M., Schrader, F., Siebicke, L., Šigut, L., Tuittila, E.-S., Varlagin, A., Vendrame, N., Vincke, C., Völksch, I., Weber, S., Wille, C., Wizemann, H.-D., Zeeman, M., and Vereecken, H.: Altered energy partitioning across terrestrial ecosystems in the European drought year 2018., *Phil. Trans. R. Soc. B*, 375, 20190524, <https://doi.org/10.1098/rstb.2019.0524>, 2022.
- 550 Haylock, M. R., Hofstra, N., Klein Tank, A. M. G., Klok, E. J., Jones, P. D., and New, M.: A European daily high-resolution gridded data set of surface temperature and precipitation for 1950–2006, *J. Geophys. Res. (Atmospheres)*, 113, D20119, doi:10.1029/2008JD010201, 2008.
- 555 Heim, R. R.: A Review of Twentieth-Century Drought Indices Used in the United States, *Bull. Amer. Meteor. Soc.*, 83, 1149–1166, 2002.
- Heinen, M., Mulder, M., van Dam, J., Bartholomeus, R., de Jong van Lier, Q., de Wit, J., de Wit, A., and Hack ten Broeke, M.: SWAP 50 years: Advances in modelling soil-water-atmosphere-plant interactions, *Agricultural Water Management*, 298, 108883, <https://doi.org/10.1016/j.agwat.2024.108883>, 2024.
- 560 Hengl, T., Mendes de Jesus, J., Heuvelink, G. B. M., Ruiperez Gonzalez, M., Kilibarda, M., Blagotić, A., Shangquan, W., Wright, M. N., Geng, X., Bauer-Marschallinger, B., Guevara, M. A., Vargas, R., MacMillan, R. A., Batjes, N. H., Leenaars, J. G. B., Ribeiro, E., Wheeler,



- I., Mantel, S., and Kempen, B.: SoilGrids250m: Global gridded soil information based on machine learning, *PLOS ONE*, 12, 1–40, <https://doi.org/10.1371/journal.pone.0169748>, 2017.
- Hirschi, M., Mueller, B., Dorigo, W., and Senviratne, S.: Using remotely sensed soil moisture for land–atmosphere coupling diagnostics: The role of surface vs. root-zone soil moisture variability, *Remote Sensing of Environment*, 154, 246 – 252, <https://doi.org/10.1016/j.rse.2014.08.030>, 2014.
- 565 Hlavinka, P., Trnka, M., Balek, J., Semerádová, D., Hayes, M., Svoboda, M., Eitzinger, J., Možný, M., Fischer, M., Hunt, E., and Žalud, Z.: Development and evaluation of the SoilClim model for water balance and soil climate estimates, *Agricultural Water Management*, 98, 1249–1261, doi:10.1016/j.agwat.2011.03.011, 2011.
- Hodnebrog, Ø., Myhre, G., Jouan, C., Andrews, T., Forster, P. M., Jia, H., Loeb, N. G., Olivié, D. J. L., Paynter, D., Quaas, J., Raghuraman, S. P., and Schulz, M.: Recent reductions in aerosol emissions have increased Earth’s energy imbalance, *Communications Earth & Environment*, 5, 166, <https://doi.org/10.1038/s43247-024-01324-8>, 2024.
- 570 Hunt, E. D., Hubbard, K. G., Wilhite, D. A., Arkebauer, T. J., and Dutcher, A. L.: The development and evaluation of a soil moisture index, *Int. J. Climatol.*, 29, 747–759, <https://doi.org/10.1002/joc.1749>, 2009.
- Ionita, M., Tallaksen, L. M., Kingston, D. G., Stagge, J. H., Laaha, G., Van Lanen, H. A. J., Scholz, P., Chelcea, S. M., and 575 Haslinger, K.: The European 2015 drought from a climatological perspective, *Hydrology and Earth System Sciences*, 21, 1397–1419, <https://doi.org/10.5194/hess-21-1397-2017>, 2017.
- Jackson, R., Canadell, J., Ehleringer, J., Mooney, H. A., Sala, O. E., and Schulze, E. D.: A global analysis of root distributions for terrestrial biomes, *Oecologia*, 108, 389–411, <https://doi.org/10.1007/BF00333714>, 1996.
- Kendon, M., Doherty, A., Hollis, D., Carlisle, E., Packman, S., McCarthy, M., Jevrejeva, S., Matthews, A., Williams, J., Garforth, J., and 580 Sparks, T.: State of the UK Climate 2023, *Int. J. Climatol.*, 44, 1–117, <https://doi.org/10.1002/joc.8553>, 2024.
- Klein Tank, A. M. G., Wijngaard, J. B., Können, G. P., Böhm, R., Demarée, G., Gocheva, A., Milate, M., Pashiardis, S., Hejkrlik, L., Kern-Hansen, C., Heino, R., Bessemoulin, P., Müller-Westermeier, G., Tzanakou, M., Szalai, S., Pálsdóttir, T., Fitzgerald, D., Rubin, S., Capaldo, M., Maugeri, M., Leitass, A., Bukantis, A., Aberfeld, R., van Engelen, A. F. V., Forland, E., Miletus, M., Coelho, F., Mares, C., Razuvaev, V., Niepova, E., Cegnar, T., Antonio López, J., Dahlström, B., Moberg, A., Kirchhofer, W., Ceylan, A., Pachaliuk, O., 585 Alexander, L., and Petrovic, P.: Daily dataset of 20th-century surface air temperature and precipitation series for the European Climate Assessment, *Int. J. Climatol.*, 22, 1441–1453, data and metadata available at <https://www.ecad.eu>, 2002.
- KNMI: Natste 12 maanden aaneen ooit gemeten, <https://www.knmi.nl/over-het-knmi/nieuws/de-natte-lente-van-2024>, 2024.
- Kroes, J., Van Dam, J., Bartholomeus, R., Groenendijk, P., Heinen, M., Hendriks, R., Mulder, H., Supit, I., and Van Walsum, P.: SWAP version 4: theory description and user manual., Tech. Rep. 2780, Alterra-rapport-Wageningen University and Research Centre, 2017.
- 590 Kysely, J.: Trends in heavy precipitation in the Czech Republic over 1961–2005, *Int. J. Climatol.*, 29, 1745–1785, doi:10.1002/joc.1784, 2009.
- Lemus-Canovas, M., Insua-Costa, D., and Miralles, D. G.: Record-shattering 2023 Spring heatwave in western Mediterranean amplified by long-term drought, *npj Climate and Atmospheric Science*, 7, 2397–3722, <https://doi.org/10.1038/s41612-024-00569-6>, 2024.
- Lesinger, K. and Tian, D.: Trends, Variability, and Drivers of Flash Droughts in the Contiguous United States, *Water Resources Research*, 58, e2022WR032186, <https://doi.org/10.1029/2022WR032186>, 2022.
- 595 Maes, W. H., Gentine, P., Verhoest, N. E. C., and Miralles, D. G.: Potential evaporation at eddy-covariance sites across the globe, *Hydrology and Earth System Sciences*, 23, 925–948, <https://doi.org/10.5194/hess-23-925-2019>, 2019.
- Makkink, G. F.: Testing the Penman formula by means of lysimeters, *J. Int. of Water Eng.*, 11, 277–288, 1957.



- Merlone, A., Pasotti, L., Musacchio, C., Bessemoulin, P., Brunet, M., El Faldi, K., Jones, P. D., van der Schrier, G., Raspanti, A., Trewin, B.,  
600 Krahenbuhl, D., and Cerveny, R.: Evaluation of the highest temperature WMO region VI Europe (continental): 48.8°C, Siracusa Sicilia,  
Italy on August 11, 2021, *International Journal of Climatology*, 44, 721–728, <https://doi.org/10.1002/joc.8361>, 2024.
- Muñoz Sabater, J., Dutra, E., Agustí-Panareda, A., Albergel, C., Arduini, G., Balsamo, G., Boussetta, S., Choulga, M., Harrigan, S., Hersbach,  
H., Martens, B., Miralles, D. G., Piles, M., Rodríguez-Fernández, N. J., Zsoter, E., Buontempo, C., and Thépaut, J.-N.: ERA5-Land: a  
state-of-the-art global reanalysis dataset for land applications, *Earth System Science Data*, 13, 4349–4383, <https://doi.org/10.5194/essd->  
605 13-4349-2021, 2021.
- Orth, R. and Seneviratne, S. I.: Introduction of a simple-model-based land surface dataset for Europe, *Environmental Research Letters*, 10,  
044 012, <https://doi.org/10.1088/1748-9326/10/4/044012>, 2015.
- Pastorello, G., Trotta, C., and Canfora, E. e. a.: The FLUXNET2015 dataset and the ONEFlux processing pipeline for eddy covariance data,  
*Sci Data*, 7, <https://doi.org/doi:10.1038/s41597-020-0534-3>, 2020.
- 610 Pendergrass, A. G., Meehl, G. A., Pulwarty, R., Hobbins, M., Hoell, A., AghaKouchak, A., Bonfils, C., Gallant, A., Hoerling, M., Hoffmann,  
D., Kaatz, L., Lehner, F., Llewellyn, D., Mote, P., Neale, R. B., Overpeck, J. T., Sheffield, A., Stahl, K., Svoboda, M., Wheeler, M. C.,  
Wood, A. W., and Woodhouse, C. A.: Flash droughts present a new challenge for subseasonal-to-seasonal prediction, *Nature Climate  
Change*, 10, 191–199, <https://doi.org/10.1038/s41558-020-0709-0>, 2023.
- Robock, A., Vinnikov, K. Y., Srinivasan, G., Entin, J. K., Hollinger, S. E., Speranskaya, N. A., Liu, S., and Namkhai,  
615 A.: The Global Soil Moisture Data Bank, *Bull. Amer. Meteor. Soc.*, 81, 1281 – 1299, <https://doi.org/10.1175/1520->  
0477(2000)081<1281:TGSMDB>2.3.CO;2, 2000.
- Robock, A., Mu, M., Vinnikov, K., Trofimova, I. V., and Adamenko, T. I.: Forty-five years of observed soil moisture in the Ukraine: No  
summer desiccation (yet), *Geophys. Res. Lett.*, 32, L03 401, [doi:10.1029/2004GL021914](https://doi.org/10.1029/2004GL021914), 2005.
- Sanchez-Lorenzo, A., Wild, M., Brunetti, M., Guijarro, J. A., Hakuba, M. Z., Calbó, J., Mystakidis, S., and Bartok, B.: Reassessment  
620 and update of long-term trends in downward surface shortwave radiation over Europe (1939–2012), *Journal of Geophysical Research:  
Atmospheres*, 120, 9555–9569, 2015.
- Seneviratne, S. I., Lüthi, D., Litschi, M., and Schär, C.: Land-atmosphere coupling and climate change in Europe, *Nature*, 443, 205–209,  
<https://doi.org/10.1038/nature05095>, 2006.
- Seneviratne, S. I., Corti, T., Davin, E. L., Hirschi, M., Jaeger, E. B., Lehner, I., Orlowsky, B., and Teuling, A. J.: Investigating soil moisture–  
625 climate interactions in a changing climate: A review, *Earth-Science Reviews*, 99, 125–161, <https://doi.org/10.1016/j.earscirev.2010.02.004>,  
2010.
- Shah, J., Hari, V., Rakovec, O., Markonis, Y., Samaniego, L., Mishra, V., Hanel, M., Hinz, C., and Kumar, R.: Increasing footprint of  
climate warming on flash droughts occurrence in Europe, *Environmental Research Letters*, 17, 064 017, <https://doi.org/10.1088/1748->  
9326/ac6888, 2022.
- 630 Suehrcke, H., Bowden, R. S., and Hollands, K. G. T.: Relationship between sunshine duration and solar radiation, *Solar Energy*, 92, 160–171,  
[doi:10.1016/j.solener.2013.02.026](https://doi.org/10.1016/j.solener.2013.02.026), 2013.
- Tagesspiegel: Regenrekord in Deutschland: Wetterdienst registriert nasseste zwölf Monate seit Messbeginn, [https://www.tagesspiegel.de/  
wissen/regenrekord-in-deutschland-wetterdienst-registriert-nasseste-zwölf-monate-seit-messbeginn-1881-11953256.html](https://www.tagesspiegel.de/wissen/regenrekord-in-deutschland-wetterdienst-registriert-nasseste-zwölf-monate-seit-messbeginn-1881-11953256.html), 2024.
- Teuling, A. J., Seneviratne, S. I., Stöckli, R., Reichstein, M., Moors, E., Ciais, P., Luyssaert, S., van den Hurk, B., Ammann, C., Bernhofer, C.,  
635 Dellwik, E., Gianelle, D., Gielen, B., Grüwald, T., Klumpp, K., Montagnani, L., Moureaux, C., Sottocornola, M., and Wohlfahrt, G.: Con-



- trasting response of European forest and grassland energy exchange to heatwaves, *Nature Geoscience*, 3, 722–727, doi:10.1038/NGEO950, 2010.
- Teuling, A. J., van Loon, A. F., Seneviratne, S. I., Lehner, I., Aubinet, M., Heinesch, B., Bernhofer, C., Grünwald, T., Prasse, H., and Spank, U.: Evapotranspiration amplifies European summer drought, *Geophys. Res. Lett.*, 40, 2071–2075, doi:10.1002/grl.50495, 2013.
- 640 Trnka, M., Kocmánková, E., Balek, J., Eitzinger, J., Ruget, F., Formayer, H., Hlavinka, P., Schaumberger, A., Horáková, V., Možný, M., et al.: Simple snow cover model for agrometeorological applications, *Agricultural and forest meteorology*, 150, 1115–1127, <https://doi.org/10.1016/j.agrformet.2010.04.012>, 2010.
- van den Besselaar, E. J. M., Klein Tank, A. M. G., van der Schrier, G., and Jones, P. D.: Synoptic messages to extend climate data records, *J. Geophys. Res. (Atmospheres)*, 117, D07 101, doi:10.1029/2011JD016687, 2012.
- 645 van der Schrier, G., Briffa, K. R., Jones, P. D., and Osborn, T. J.: Summer moisture variability across Europe, *J. Climate*, 19, 2828–2834, 2006.
- van der Schrier, G., van den Besselaar, E. J. M., Klein Tank, A. M. G., and Verver, G.: Monitoring European averaged temperature based on the E-OBS gridded dataset, *J. Geophys. Res. (Atmospheres)*, 118, –, doi:10.1002/jgrd.50444, 2013.
- van der Schrier, G., Allan, R. P., Ossó, A., Sousa, P. M., Van de Vyver, H., Van Schaeybroeck, B., Coscarelli, R., Pasqua, A. A., Petrucci, O., 650 Curley, M., Mietus, M., Filipiak, J., Štěpánek, P., Zahradníček, P., Brázdil, R., Řezníčková, L., van den Besselaar, E. J. M., Trigo, R., and Aguilar, E.: The 1921 European drought: impacts, reconstruction and drivers, *Clim. Past*, 17, 2201–2221, doi:10.5194/cp-17-2201-2021, 2021.
- van der Schrier, G., Fischer, M., Mulder, M., van Dam, J., Řehoř, J., and Trnka, M.: Dataset of daily soil moisture from *in situ* meteorological observations, *European Climate Assessment & Dataset*, <https://doi.org/10.21944/phk8-at71>, 2026.
- 655 van der Wiel, K., Batelaan, T., and Wanders, N.: Large increases of multi-year droughts in north-western Europe in a warmer climate, *Climate Dyn.*, 60, 1781–1800, <https://doi.org/10.1007/s00382-022-06373-3>, 2023.
- Whan, K., Zscheischler, J., Orth, R., Shongwe, M., Rahimi, M., Asare, E., and Seneviratne, S. I.: Impact of soil moisture on extreme maximum temperatures in Europe, *Weather and Climate Extremes*, 9, 57–67, <https://doi.org/10.1016/j.wace.2015.05.001>, 2015.
- Wigley, T. M. L. and Atkinson, T. C.: Dry years in south-east England since 1698, *Nature*, 265, 431–434, 1977.
- 660 WMO: Manual on the Global Telecommunication System, Geneva, Ch, wmo-no. 386 edn., 2007.
- WMO: WMO Unified Data Policy Resolution (Res. 1), <https://public.wmo.int/en/our-mandate/what-we-do/observations/Unified-WMO-Data-Policy-Resolution>, 2022.
- WMO: The Rolling Review of Requirements process, <https://public.wmo.int/en/our-mandate/what-we-do/observations/Unified-WMO-Data-Policy-Resolution>, 2023.
- 665 Wösten, J., Lilly, A., Nemes, A., and Le Bas, C.: Development and use of a database of hydraulic properties of European soils, *Geoderma*, 90, 169–185, [https://doi.org/10.1016/S0016-7061\(98\)00132-3](https://doi.org/10.1016/S0016-7061(98)00132-3), 1999.
- Yuan, X., Wang, Y., Ji, P., Wu, P., Sheffield, J., and Otkin, J. A.: A global transition to flash droughts under climate change, *Science*, 380, 187–191, <https://doi.org/10.1126/science.abn6301>, 2023.
- Zolina, O., Simmer, C., Gulev, S. K., and Kollet, S.: Changing structure of European precipitation: Longer wet periods leading to more 670 abundant rainfalls, *Geophys. Res. Lett.*, 37, L06 704, doi:10.1029/2010GL042468, 2010.
- Řehoř, J., Trnka, M., Brázdil, R., Fischer, M., Balek, J., van der Schrier, G., and Feng, S.: Global hotspots in soil moisture-based drought trends, *Environ. Res. Lett.*, 19, 014021 483, <https://doi.org/10.1088/1748-9326/ad0f01>, 2024.